JACS
JOURNAL OF THE AMERICAN CHEMICAL SOCIETY
pubs.acs.org/JACS
Perspective

Methanol to Olefins (MTO): Understanding and Regulating Dynamic Complex Catalysis

Shanfan Lin,[⊥] Hua Li,[⊥] Peng Tian, Yingxu Wei,* Mao Ye,* and Zhongmin Liu*

Cite This: J. Am. Chem. Soc. 2025, 147, 11585−11607
Read Online
ACCESS | Metrics & More | Article Recommendations

ABSTRACT: The research and development of methanol conversion into hydrocarbons have spanned more than 40 years. The past four decades have witnessed mutual promotion and successive breakthroughs in both fundamental research and industrial process development of methanol to olefins (MTO), demonstrating that MTO is an extremely dynamic, complex catalytic system. This Perspective summarizes the endeavors and achievements of the Dalian Institute of Chemical Physics, Chinese Academy of Sciences, in the continuous study of reaction mechanisms and process engineering of the dynamic, complex MTO reaction system. It elucidates fundamental chemical issues concerning the essence of the dynamic evolution of the MTO reaction and the cross-talk mechanisms among diffusion, reaction, and catalyst (coke modification), which are crucial for technology development and process optimization. By integrating the chemical principles, the reaction-diffusion model, and coke formation kinetics of MTO, a mechanism- and model-driven modulation of industrial processes has been achieved. The acquisition of a deepening understanding in chemistry and engineering has facilitated the continuous optimization and upgrading of MTO catalysts and processes.

1. INTRODUCTION

Methanol, a key C1 platform compound producible from coal, natural gas, biomass, organic waste, and carbon dioxide, has attracted long-term and extensive attention from both academia and industry, as it can be further transformed into a diverse array of fuels and chemicals.[1−24] Oil has historically spurred human societal development and unprecedented prosperity by providing fuels and basic chemicals. However, with the increasing energy demand and dwindling oil resources, intertwined with the requirement for green, low-carbon global transition to address climate change, the efficient conversion of nonoil resources, especially using methanol as a bridge, has emerged as a crucial pathway.[25−28] Long-term, extensive efforts from many institutions and companies, particularly those key contributors, have been devoted to research in zeolite-catalyzed methanol conversion, and significant progress has been achieved in the reaction principles[1−24,29−31] (supported by the breakthroughs in advanced *in situ/operando* spectroscopy,[4,5,29−42] theoretical simulations,[14,43−47] and characterization techniques[29−31,45,48,49]), catalyst synthesis,[1,23,50−59] and process industrialization.[1,60−66]

Methanol can be converted into hydrocarbon-based fuels and chemicals over acid zeolite catalyst featured with shape-selectivity via a variety of methanol-to-hydrocarbons (MTH) reactions, encompassing methanol-to-olefins (MTO), methanol-to-propene (MTP), methanol-to-aromatics (MTA), and methanol-to-gasoline (MTG).[1−24,29−31] Among them, MTO have achieved successive breakthroughs in both fundamental research and process industrialization, fostering mutual promotion (as outlined in Figure 1) since its first discovery[67] in 1977.[1−24,29−31,60−66] The team at the Dalian Institute of Chemical Physics (DICP), Chinese Academy of Sciences, has been dedicated to research and development (R&D) of MTO process for more than 40 years since the 1980s, and has achieved a series of innovations and inventions in reaction mechanisms, catalyst synthesis, process engineering, and industrialization, which ultimately have led to the development of a series of commercial DMTO technologies[1,60] for massive production of light olefins from nonoil resources. In 2010, the world's first industrial coal-to-olefins plant had been constructed and started up in Baotou, Inner Mongolia, by use of DMTO technology after the successful pilot plant (300t/a methanol feed, in 1995) and industrial demonstration unit (16 kt/a methanol feed, in 2006) tests. This marks a significant milestone for commercial production of ethylene and propylene from nonoil resources. In a previous Perspective,[1] we have documented the story concerning our work from fundamental research to industrialization of the first-generation DMTO technology. In 2014, the second-generation technology, i.e., DMTO-II, characterized by the recycling of C_4^+ byproducts into an extra fluidized bed cracking reactor to increase the ethylene and propylene yields, was industrialized at Pucheng, Shaanxi. DICP has continuously innovated to develop the third-generation MTO technology (DMTO-III), grounded in a profound principle comprehension of the reaction mechanisms, catalyst selectivity, multiscale reaction-diffusion, and reactor coke distribution. The DMTO-III

Received: September 2, 2024
Revised: March 7, 2025
Accepted: March 7, 2025
Published: March 26, 2025

https://doi.org/10.1021/jacs.4c12145
J. Am. Chem. Soc. 2025, 147, 11585−11607

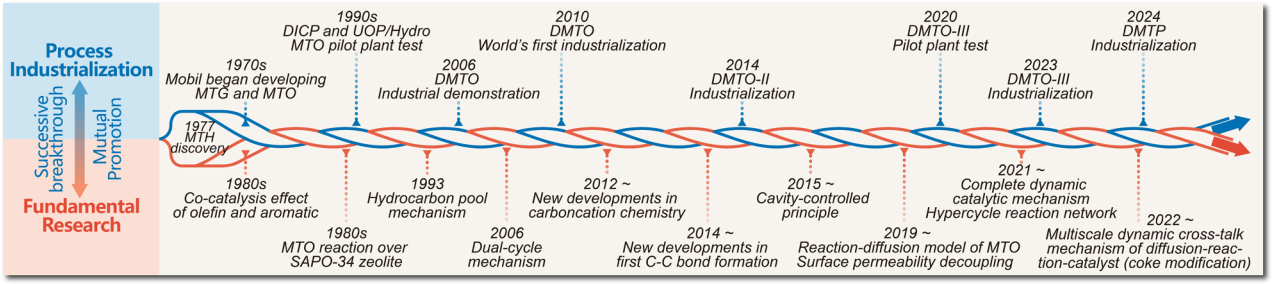

Figure 1. Milestones and mechanism development of the MTO process.

technology, which is based on the new-generation DMTO catalyst and a highly efficient fluidized bed reactor, can achieve the methanol feed rate up to 4.0 Mt/a by use of a single industrial reactor, with a methanol to light olefins ratio of 2.66 t/t. The first DMTO-III industrial unit was commissioned in August 2023 at Yinchuan, Ningxia. So far, the DMTO series technologies have been licensed to 36 industrial units, with 18 units coming into stream. Very recently, the DMTP technology, an alternative to DMTO, has also been licensed for the construction of an industrial unit in Yulin, Shaanxi. In the future, guided by the multienergy integration technology system,[28] a coal-to-olefins (CTO) integrating green hydrogen process is being developed under "Dual Carbon" goals, potentially reducing CO_2 emissions by nearly 70%—compared to the typical CTO process, in which 97% of emissions are derived from coal gasification and methanol synthesis as evaluated by life cycle assessment (LCA).

The discovery of the MTO reaction and thriving industrialization of the MTO process have significantly inspired and sparked a series of pivotal advancements in fundamental research. Many scientific issues have attracted shared interests in both fundamental research and industrial process development of the dynamic and complex MTO process:

1 What is the detailed mechanism underlying the catalytic reaction throughout the entire catalyst lifetime, encompassing the first C−C bond formation, induction stage, autocatalysis, olefin formation, coking, and deactivation?
2 How to mitigate or avoid the unexpected reaction stages such as induction stage, deactivation, and control the reaction toward maximum olefin selectivity and minimal coking rate?
3 How to describe and model the dynamic complex reaction system coupled with diffusion?
4 How to regulate the reaction, coke deposition, and diffusion to achieve an efficient MTO process technology?

The unremitting exploration into these issues has driven the advancement of fundamental research in MTO processes. Direct and indirect mechanisms have been sequentially proposed to understand the methanol conversion pathways. Although the direct mechanism was initially proposed, it has only undergone significant development since 2014, supported by advanced *in situ* spectroscopy and theoretical calculations, leading to the proposal of various direct coupling pathways (particularly the coupling of surface methoxy species (SMS) with other C1 species), which greatly enriched the understanding of the first C−C bond formation mechanisms.[38,68−84] The failure of the direct mechanism to explain the observed autocatalysis behavior, the S-shaped kinetic profile and induction period,[28,34−37] prompted the proposal of indirect mechanisms. Guided by autocatalytic attribute,[85] the co-catalysis effect of olefins[86,87] and aromatics,[88,89] and the concept of "hydrocarbon pool (HCP)"[90−92] were proposed successively. Moreover, the identification and capture (especially directly under real reaction conditions) of HCP species, particularly carbocations, along with the establishment of catalytic cycles through isotopic labeling combined with theoretical calculations, have greatly advanced the development of indirect mechanisms as well as carbocation chemistry.[8,29,93−105] From the proposal of the olefin methylation-cracking mechanism[86,87] to the dual-cycle mechanism (olefins- and aromatics-based cycle),[106−108] and then to the three-cycle mechanism (dual-cycle and MCP-based cycle),[109,110] the indirect mechanisms have progressed from a single catalytic cycle to a hypercycle[80] reaction network with multiple catalytic cycles operating concurrently and cooperatively, effectively explaining the generation of target olefins generation during the high-efficient stage. With those active organic species involved in the hypercycle inevitably decaying and aging into on-surface or in-pore inactive polycyclic aromatic hydrocarbons (PAHs) as coke, the catalyst gradually deactivates.[80,111,112] Considering all catalytic events comprehensively, we established a complete autocatalysis mechanism[80] to describe the entire dynamic process of methanol conversion from the initiation to the decay. Concurrently, we established the principle of cavity-controlled shape-selective catalysis,[20] together with cross-talk mechanism of diffusion-reaction-material,[113] tailored for the industrial application of eight-membered ring (8-MR) and cavity-type zeolites catalytic systems, which offers an important strategy for controlling the MTO reaction catalyzed by zeolites. As a typical heterogeneous catalytic process, in addition to the dynamic complex reaction system, an understanding of the reaction-diffusion mechanism is also highly desired. Notably, coke deposition not only causes catalyst deactivation but also leverages the optimal shape-selectivity properties of the catalyst.[114] Therefore, it is essential to control the coke distribution at both the zeolite catalyst scale and the reactor scale to optimize the light olefin selectivity in the MTO process. By developing a kinetic model,[115−117] decoupling and directly quantifying surface permeability and intracrystalline diffusivity,[118,119] we have established the reaction-diffusion mechanism and a quantitative model of the MTO reaction.[116,117,120] The established quantitative description of reaction-diffusion at the zeolite catalyst scale is consequently implemented into a reactor scale coke distribution balance equation to modulate the industrial MTO processes.[114]

https://doi.org/10.1021/jacs.4c12145
J. Am. Chem. Soc. 2025, 147, 11585−11607

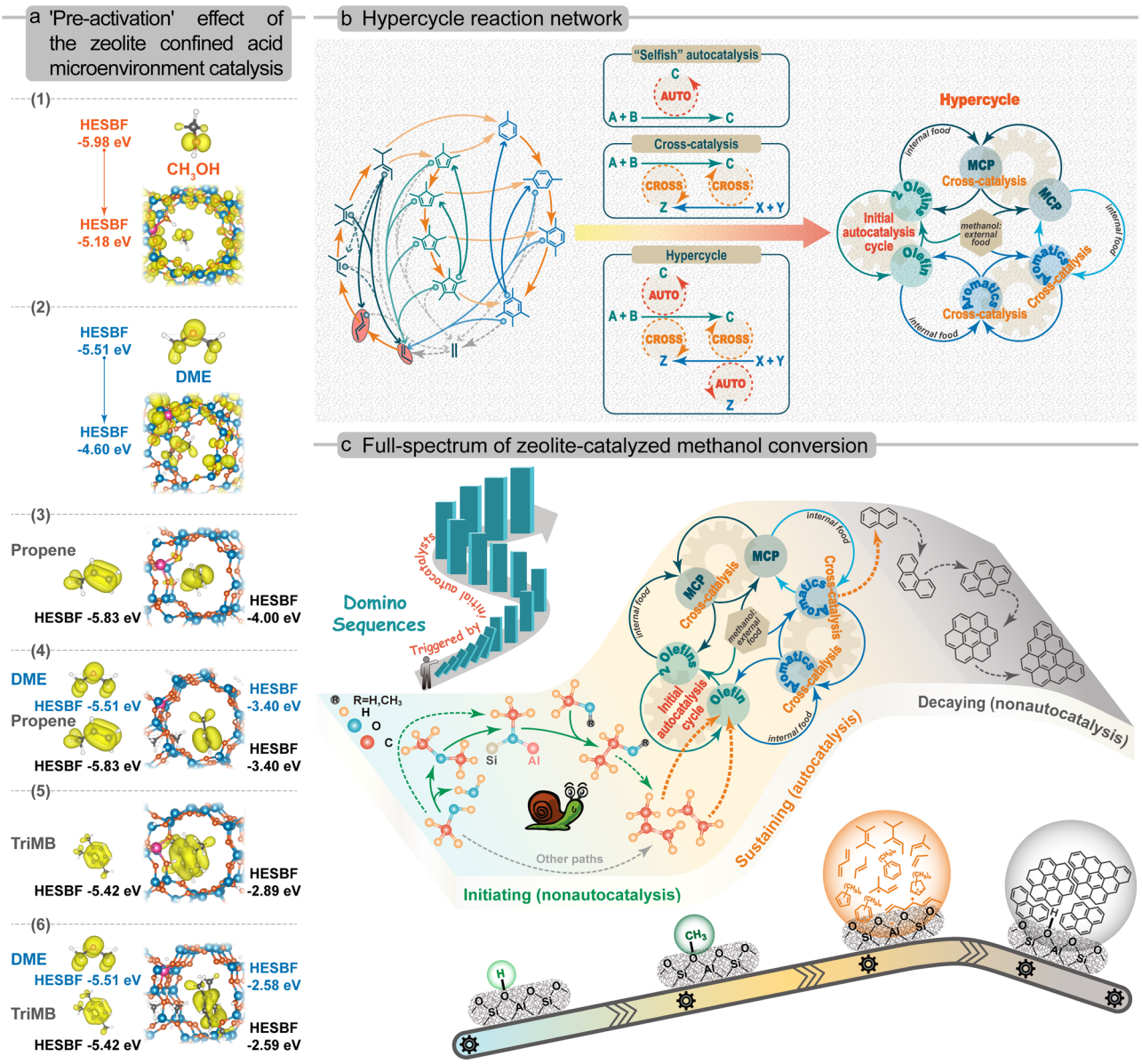

Figure 2. (a) The energies of HESBF for methanol, DME, propene, triMB and their respective complexes with DME in gas phase and in zeolite confined space. (b) Hypercycle reaction network. The autocatalytic sets, operating by a hypercyclic network embedded in the large interlinked network, interlinked by three autocatalytic entities (olefin, MCP and aromatic species), driving the autocatalytic turnover. The concept of the figure is based on refs [80] and [130]. (c) Full-spectrum molecular routes of a domino cascade reaction network for zeolite-catalyzed methanol conversion. A full molecular picture of the MTH reaction network with diverse and cooperative catalytic and autocatalytic events associated with the dynamic restructuring of active sites along the evolutionary trajectory. Adapted from ref [80]. Copyright 2021 American Chemical Society.

Throughout this continuous MTO research endeavor, we are always facing extremely dynamic complex systems with numerous challenges. Exploration of the above key scientific questions has greatly expanded and deepened our understanding of the fundamental catalytic principles of MTO, which form the cornerstone for the optimization and development of MTO catalysts and processes and promote the upgrading of MTO industrial technology.

In this Perspective, we will comprehensively summarize our endeavors and achievements made in addressing the challenges associated with the understanding of dynamic complex MTO chemistry, the establishment of reaction-diffusion mechanisms and quantitative models, and the regulating and optimizing of coke distribution in industrial process. From the first C−C bond generation to the efficient conversion of methanol to light olefins through the hypercycle network and further to deactivation, we have elucidated the dynamic reaction evolution and the underlying reaction mechanisms hidden within the MTO process. By establishing the cross-talk mechanism of diffusion-reaction-catalyst (coke modification) and constructing the reaction-diffusion kinetic models, we achieved the regulation and upgrading of MTO industrial processes driven by fundamental principles and kinetics modeling. Based on the zeolite acid catalysis theories, shape-selectivity modulation principles, and practical reaction control strategies in MTO, we will envision the future innovations and development directions of MTO mechanisms, catalysts, and industrial processes. This MTO research is expected to contribute to the broader development of zeolite catalysis theories applicable to dynamic and complex reaction systems.

https://doi.org/10.1021/jacs.4c12145
J. Am. Chem. Soc. 2025, 147, 11585−11607

2. DYNAMIC MECHANISM OF MTO

2.1. Full-Spectrum of MTO: Dynamic Autocatalysis Process from Initiation to Decay. Zeolite-mediated catalytic conversion of methanol is a dynamic C−C bond assembly process within a confined acid microenvironment of zeolite, from C1-feedstocks to a diverse array of multicarbon hydrocarbons, which span alkenes, aromatics, alkanes, polycyclic aromatics, and oxygen-containing compounds, vary in carbon numbers and unsaturation degrees, present in both gas effluent and zeolite interface. Mechanism of these C−C bonds construction, especially the generation of the first C−C bond and the target olefin product, has always been the most critical scientific issue since the discovery of the MTH reaction in the 1970s.[1,2,7,12] Generally, two categories of mechanisms, direct mechanism and indirect mechanism, have been proposed to shed light on this issue. Throughout the history of MTH research, studies of the two mechanisms have developed alternately, ultimately providing a comprehensive understanding of the methanol conversion mechanism.

In the early research of the last century, more than 20 direct mechanisms[3] were proposed to explain the pathways of methanol conversion, but all were identified as infeasible due to either a lack of reliable experimental evidence or prohibitively high energy barrier from a theoretical standpoint.[1,2,7,12,121] These impediments led to stagnation in direct mechanisms until recent years[12] when it experienced a renaissance, providing many first C−C bond building routes[38,68−84] thanks to the development of advanced spectroscopic techniques and theoretical calculations. We argue this controversial issue from the perspective of the dynamic activation and transformation of two C1 reactant molecules, methanol and dimethyl ether (DME), under the real reaction conditions and zeolite local microenvironments during the initial stage of methanol conversion, emphasizing the critical importance of meticulously obtaining pertinent evidence under these real specific conditions.

Our recent findings uncover that, in fact, the zeolite catalysis for such an intricate MTH catalytic process starts with the "pre-activation" effect[80] of guest molecules (Figure 2a), evoked by the confined acid microenvironment of zeolite: as methanol and DME diffuse from gas phase into zeolite confined spaces, their highest electronic states below Fermi-level (HESBF)[80] increase, getting ready for subsequent catalysis. Two C1 species need to be activated and then react by direct coupling to construct the first C−C bond. The SMS, formed upon adsorption of methanol/DME on Brönsted acidic sites (BASs), also including SMS bound to extra-framework Al,[75,76] have been generally acknowledged and verified as a key intermediate, serving as one of the active C1 species with various specific functional modes in most of the recently proposed pathways for the first C−C bond formation,[68−82] including our works.[73,77,80−82] For another active C1 species, both our kinetic studies and theoretical calculation (showing marked pre-activation of DME than methanol) evidence that DME, the dehydration product of methanol, is a more reactive C1 species than methanol.[80] Furthermore, 2D $^{13}C-^{13}C$ NMR spectroscopy[77,80] combined with projected density of state (PDOS) calculation[80] analysis successfully reveal the spatial proximity/correlation and electronic interaction between the two active C1 species—the SMS and DME, leading to the activation of the C−H bond of DME by the synergetic effect of SMS and adjacent framework oxygen. Remarkably, *in situ* solid-state MAS NMR spectroscopy at programmed temperatures directly observed this dynamic activation process of DME,[82] evolving from the adsorption state to the activated state—the methyleneoxy analogue species ($CH_3-O-CH_2^{\delta-}—H^{\delta+}$),[73] which were first captured *in situ* within a working catalysts during the initial stage of methanol conversion.[73] Concomitantly, *ab initio* molecular dynamics (AIMD) simulations demonstrate that the C−O bond of the SMS transforms from covalent-bonding to ionic-bonding with increasing temperature.[82] Consequently, the activated DME ($CH_3-O-CH_2^{\delta-}—H^{\delta+}$) and the activated SMS with the positively charged methyl group ($CH_3^{\delta+}$) are ready for C−C coupling. *Operando* AIMD simulations further detailed and visualized the dynamic activation and direct coupling reaction process.[80] When DME/methanol approached the SMS, collisions/interactions stretched the C−O bond of the SMS and the C−H bond of DME/methanol was elongated with the assistance of framework oxygen. C−C bond formed synchronously by the nucleophilic attack of DME/methanol with the SMS. C−C bond formation was paralleled with C−H bond breakage; these processes coincided with (for methanol) or after (for DME), C−O bond ionization of the SMS. Finally, proton H (originating from the broken C−H) is donated back to the negatively charged framework O to recover the BASs of zeolite. The minimal energy pathways on two-dimensional free energy surface demonstrated that free-energy barrier (154 kJ/mol) for the SMS-mediated DME pathway was lower than that (184 kJ/mol) for the SMS-mediated methanol pathway for generating first C−C bond containing species.[80]

After constructing the first C−C bond-containing species via direct mechanism of methanol conversion, the incipient olefins, mostly ethene and/or propene, will quickly generate from these species on the catalyst surface, and work as the initial autocatalysts to initiate the autocatalytic reaction via olefins-based cycle,[80] which is the dominant autocatalytic cycle in the induction stage of MTH reaction.[80,99,122] In this manner, the indirect mechanism of methanol conversion is triggered by a direct mechanism. Essentially, the indirect mechanism represents the autocatalytic reaction of methanol with hydrocarbon species (functioning as autocatalysts), which is a more energetically favorable and efficient pathway. Originating from this, catalysis evolution from direct to indirect mechanisms, with the indirect mechanism becoming dominant, inherently results in a lower initial conversion rate of methanol, manifesting the key characteristic known as the "kinetic induction period". Our recent work[22] revisits the chemical nature of the autocatalytic induction period in methanol conversion, which stems from kinetically sluggish generation and accumulation of initial autocatalysts attributed to the intricate and low-activity of initial local catalytic microenvironments. Historically, the autocatalytic attribute[85] of methanol conversion, unveiled shortly following the discovery of the MTH reaction,[67] together with the induction period characteristic, have laid a solid foundation for understanding the mechanism of methanol conversion. Centered on autocatalytic attribute, the development of indirect mechanism flourished: the co-catalysis effect of olefins (olefin methylation-cracking mechanism)[86,87] and aromatics,[88,89] the hydrocarbon pool concept,[90−92] the dual-cycle mechanism,[106−108] and the three-cycle mechanism[56,57] were subsequently proposed.

The complexity and specificity of methanol conversion process primarily stem from its unique autocatalytic nature,

https://doi.org/10.1021/jacs.4c12145
J. Am. Chem. Soc. 2025, 147, 11585−11607

manifested as a dynamic autocatalysis process occurring within confined acid microenvironments of zeolite, in stark contrast to classic autocatalytic reactions[123,124] that generally occur in open spaces and involve fixed autocatalysts. Autocatalysts dynamically evolve from initial olefins into a diverse series of cyclic species, such as polymethylcyclopentadienes (MCPs) and polymethylbenzenes, which in turn generate novel autocatalytic pathways, continuously altering and enriching the methanol conversion pathway and network, leading to the construction of a dynamic, complex, and diverse set of indirect mechanisms. As these highly active hydrocarbon autocatalyst species are generated and accumulate, the indirect mechanism progressively matures, developing into the dominant pathway for methanol conversion and target olefin production during the highly efficient reaction stage. This process exerts a dual acceleration effect on methanol conversion due to both dynamic autocatalysis and nanoconfinement,[125−127] representing the combination of guest-mediated and host-mediated accelerated chemical reactions in one, with a particular emphasis on the autocatalysis acceleration effect driven by the simultaneous enhancement of both the activity (dynamic autocatalysis) and quantity of the autocatalyst. Correspondingly, the kinetic behavior of methanol conversion exhibits a sigmoidal kinetic profile,[80,85,128] characterized by a kinetically sluggish initial stage followed by a rapid ascending period, enabling exponential propagation of autocatalytic turnover. Intriguingly, the diverse indirect mechanisms share a unifying chemical (or autocatalysis) principle that can be succinctly described as follows:[109,113,129] methanol/DME gradually methylate with the active intermediates (acting as autocatalysts) to form the extended entities (olefins precursors), from which light olefins are subsequently generated by cracking or elimination reactions, simultaneously completing the autocatalytic cycle. The identified active intermediates, including carbocations and their corresponding neutral species,[8,29,93−105] exhibit diversity, mainly encompassing olefinic, MCP, and aromatic species, each independently guiding olefins-based cycle,[106−108] MCP-based cycle[109] and aromatics-based cycle,[106−108] respectively. These catalytic cycles exhibit a unified attribute of autocatalysis, collectively forming complex reaction networks/patterns. By virtue of classic autocatalysis concept,[130] we disentangled the chemical nature of the convoluted autocatalytic reaction network, which is distinctly identified as a "hypercycle"[80] (Figure 2b): being cooperatively constituted by "selfish" autocatalysis cycle (i.e., olefins-based cycle with lighter olefins as autocatalysts for catalyzing the formation of themselves) and cross-catalysis cycles (with olefins, MCP and aromatic species as autocatalysts for catalyzing each other's formation), efficiently driving and sustaining the autocatalysis of methanol and DME conversion.

However, those active HCP species, generated from initial olefin conversion, simultaneously sustain highly efficient autocatalytic methanol conversion (acting as co-/autocatalysts) while inevitably continue to undergo dynamic evolution (acting as coke precursors), extending the C−C bond assembly process and aging into confined PAHs located on the internal and/or external surface of the catalyst, including naphthalene, fluorene, phenanthrene, pyrene, and even larger cross-linked cage-passing multicore aromatic[111,112] species, directly leading to the loss of active centers for MTO. The two processes involving active HCP species with dual roles appear to be competitive, with the latter thermodynamically favored,[8,31] representing the thermodynamic driving force toward catalyst inevitable deactivation. Naphthalenes are generally regarded as inactive HCP species at relatively low reaction temperatures, but exhibit high-temperature activity,[131] enabling the naphthalene-based cycle[132,133] and favoring ethylene production.[131−135] Phenanthrenes and more condensed PAHs typically struggle to sustain the autocatalytic cycle while simultaneously covering active sites and occluding the catalyst pores or cages, causing severe diffusion limitations for reactants (acting as inactive bad coke). Moreover, these inactive heavier PAHs coke are typically located at the out surface of zeolite crystal, such as the external surface[31,48,107,136−142] of ZSM-5 (also located at internal (intersection and straight channels) surface,[31,139−144] both contribute to ZSM-5 deactivation[31,137−144]), or in near-surface regions, such as the rim/outer-shell cages of SAPO-34, as directly imaged by super-resolution structured illumination microscopy (SIM),[113,120] 3D using multilaser excitation confocal fluorescence microscopy (CFM),[138,145,146] atom probe tomography (APT),[147−149] combined in situ UV/vis and synchrotron-based IR microscopy (IRM),[150] and characterized by matrix-assisted laser desorption/ionization Fourier-transform ion cyclotron resonance mass spectrometry (MALDI FT-ICR MS),[111,112] laser desorption/ionization (LDI)−TOF MS[141] and EELS.[139] Such coke spatial distribution further hampers the accessibility and utility of the active sites and activated intermediates within the internal near-core part of the crystal. Ultimately, these factors—active center directly decay and/or reduced accessibility due to diffusion limitations evoked by coke deposition—result in the termination of the dynamic autocatalysis and the C−C bond assembly process, as well as catalyst deactivation.

Together, a full-spectrum of molecular routes for the domino cascade of methanol dynamic catalytic process and network occurring within the confined acid microenvironments of zeolite is mapped (Figure 2c).[80] The reaction sequence runs from the initiation (the establishment of incipient autocatalysts), to sustaining (the operation of hypercycle network), and to decay (the extinction of autocatalysis) like domino. The reaction of DME, a distinctly verified, more active C1 species (relative to methanol), with SMS is validated as the more plausible mechanistic pathway to generate the first C−C bond and initial olefins. Despite the substantial evidence gathered, this is by no means conclusive (or exclusive), as other conceivable initial C−C bond building routes[38,68−84] may also exist and operate. The formed initial olefins function as the "switch" to trigger the autocatalysis and drive the efficient conversion of methanol by gradually forming confined HCP species, including MCP and aromatic cyclic organics, which collectively build the hypercycle network,[80] and continue to form confined inactive PAHs, in the process transforming the organic-free zeolite catalyst into a working catalyst, and eventually into a deactivated catalyst. Correspondingly, the MTO reaction experiences an induction stage, a high-efficient stage, and a deactivation stage. In the context of various zeolite confined microenvironments and by dealing with the effect of zeolite pore space, acidity, and reaction conditions, the autocatalytic cycles/network are unified as the generalized hypercycle with diverse molecular routes. At every moment during the reaction, the catalytic system, comprising confined organic species and the zeolite microenvironment, undergoes dynamic progression, corresponding to a continuously evolving reaction network and product generation. As a result, in the methanol conversion, there is no true steady-state

https://doi.org/10.1021/jacs.4c12145
J. Am. Chem. Soc. 2025, 147, 11585−11607

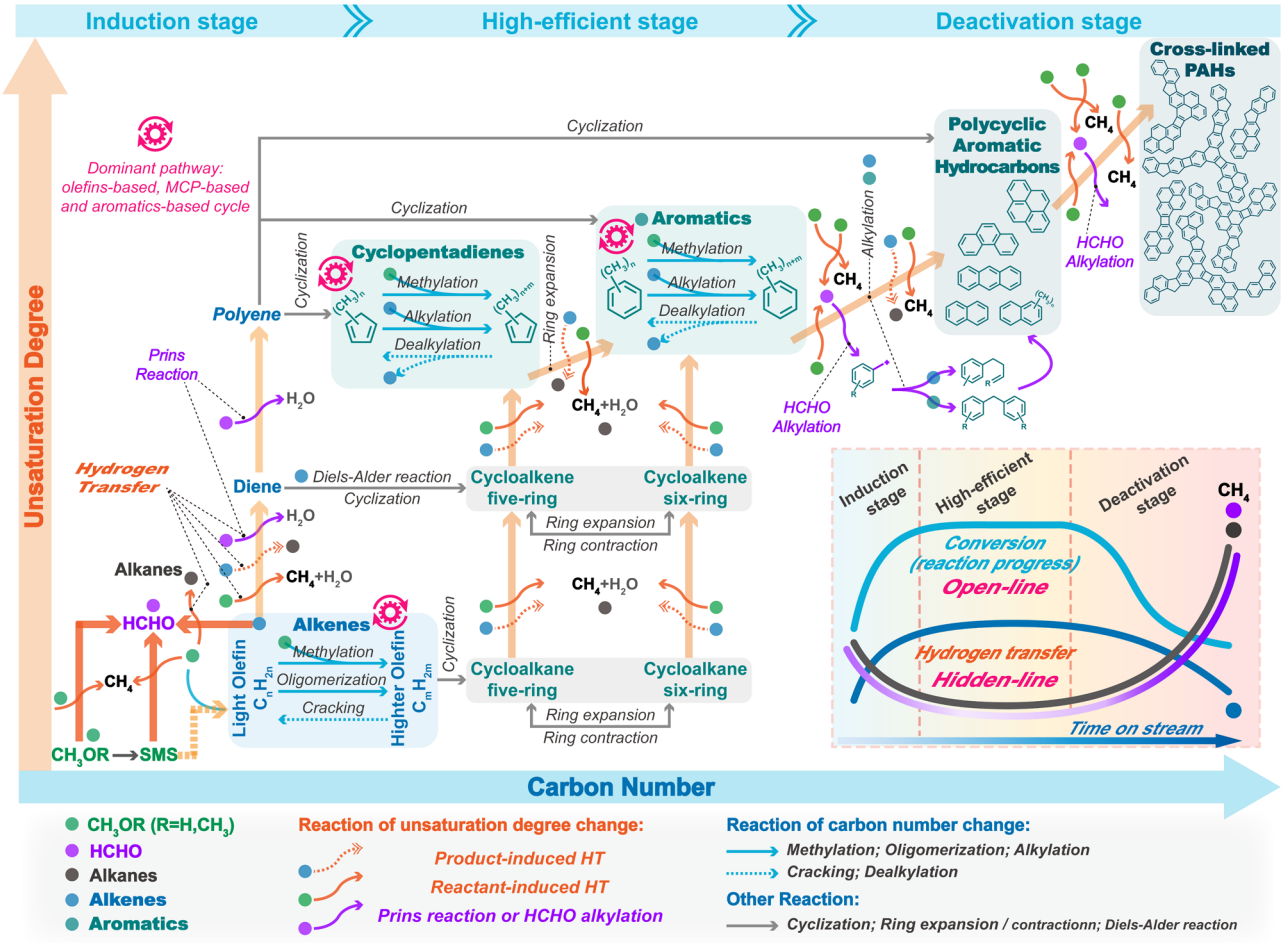

Figure 3. Reaction network of zeolite-catalyzed methanol to hydrocarbon process. Adapted with permission from ref [154]. Copyright 2023 Elsevier.

reaction stage but rather a high-efficient stage driven by the hypercycle.

Concurrent with the dynamic development of the methanol conversion from initialization to high efficiency is the relay generation and functioning of the active centers, which evolve from acidic protons to the SMS, and then to organic-confined zeolite microenvironment active centers—the true active centers to drive the autocatalysis. Correspondingly, catalysis of zeolite-catalyzed methanol conversion extends beyond the traditional BAS catalysis category,[21] and the highly efficient methanol conversion is achieved through the catalysis by the combination of the generated organic substances and the confined acid microenvironment.[80] We refer to this as organic-confined zeolite microenvironment catalysis. In 2005, Haw et al.[151] introduced the concept of "zeolite supramolecule catalyst", emphasizing that inorganic zeolite and organic HCP species do not function independently but rather hybridize together to form a supramolecule catalyst that serves as the active center of typical MTO working catalysts. Our proposal of organic-confined zeolite microenvironment catalysis, taking another step forward in understanding active centers and zeolite catalysis, emphasizes the crucial importance of the local confined microenvironment of zeolites in the actual MTH catalytic process, which is mainly reflected in two aspects: (i) The "pre-activation" effect[80] of guest molecules arises from the electron confinement effect[152,153] conferred by the zeolite confined acid microenvironment (Figure 2a), as confirmed and quantified by HESBF energy analysis. Notably, relative to in gas phase, the HESBF energies increased by 0.91, 2.11, and 2.93 eV, respectively, for DME in the confined acid microenvironment of HZSM-5, the propene-confined microenvironment of HZSM-5, and the trimethylbenzene-confined microenvironment of HZSM-5.[80] The HESBF energies of propene and trimethylbenzene are also elevated in the confined acid microenvironment of HZSM-5, with pre-activated olefin and aromatics tending to undergo electrophilic substitution reactions, such as methylation, to propagate autocatalytic chains. Dynamic organic-confined zeolite microenvironment catalysis gradually intensifies the "pre-activation" effect of DME, as evidenced by the progressively elevated HESBF energies, which correspond to an increase in basicity[153] of the confined molecules that favors electron transfer; (ii) The significant impact of the local chemical potential of reactants and products (enrichment or depletion in local concentration) within the confined acid microenvironment of zeolite on methanol conversion.[113,154]

In summary, these discoveries and perspectives have unveiled the complexity and dynamism of MTO reaction systems. Understanding the complete dynamic autocatalysis mechanism has been instrumental in achieving an efficient and stable MTO process.

2.2. Hidden Line of MTO: Ever-Evolving Organic Species from Generation to Aging within Zeolite Confined Acid Microenvironment. The dynamic autoca-

https://doi.org/10.1021/jacs.4c12145
J. Am. Chem. Soc. 2025, 147, 11585−11607

talysis process of methanol conversion manifests as a characteristic S-shaped kinetic curve from initiating to sustaining, transitioning into an inverse S-shaped curve from sustaining to decaying. This S-shaped plus (upward) inverse S-shaped (downward) curve, the most striking kinetic behavior of MTO reaction, serves as the "open-line" of MTO, classically dividing the dynamic process into three well-known successive reaction stages, including induction stage, high-efficient stage, and deactivation stage. The "open-line" of MTO[154] represents the primary reaction for the target olefin production in MTO, driven by the established hypercycle reaction network involving active organic species. Beneath the "open-line", MTO dynamic catalysis process is guided by the ever-evolving organic species within the confined microenvironment of zeolite, encompassing the formation of active organic species and their evolution into inactive PAHs species.[80,154] Accordingly, we proposed that the ever-evolving organic species within the zeolite confined microenvironment from generation to aging serves as the "Hidden line" of MTO.[154] We introduced the concepts of the "Open-line" and "Hidden-line" to capture the most prominent and significant features of the highly complex MTO process, providing a clear and accurate representation of its dynamic behavior and nature. The "Open-line" and "Hidden-line" simultaneously occur and interplay, constituting the complete dynamic reaction network and process of MTO (Figure 3).[154]

The full dynamic evolution of organic species within zeolite confined acid microenvironment, from their generation to aging, is also illustrated in Figure 3.[154] This process starts with the simplest C1 reactants and progresses through the formation of the first C−C bond, initial olefins, aromatics, naphthalene, and eventually PAHs, evolving in a domino-like manner toward increasing carbon numbers and unsaturation, with both near-linear and discrete leaps in growth. Initial olefins, derived from the first C−C bond-containing species,[38,68−84] undergo continuous methylation to yield a series of alkenes, in which higher alkenes crack into light olefins, completing the olefins-based cycle.[106−108] Alkenes also undergo intermolecular HT reactions to form alkanes and dienes, or react with methanol to produce alkanes and formaldehyde.[11,141,154−156] It is generally accepted that initial cyclic organic species, including cycloalkanes and cycloalkenes with three-, five-, or six-membered rings, are generated from initial olefins via a series of reactions, such as oligomerization, cyclization, and hydrogen transfer (HT), and they can also interconvert through ring contraction, ring expansion, HT and methylation reactions.[28,30−32,154,157,158] In recent years, the mechanism of initial aromatic generation has been enriched. Substantial experiments evidenced that methylcyclopentenyl cations (MCP^+) formed preferentially over aromatics and could transform into them.[99,103] Methylcyclohexene (MCH) is confirmed as a key species with high reactivity to establish initial MCP and aromatics species, in which it tends to form MCP via ring contraction and HT, followed by ring expansion to form aromatics.[159,160] As for the generation of MCH, Diels−Alder reaction between dienes and monoenes is proposed as a more energetically feasible route than oligomerization and cyclization of alkenes.[160] In addition, another route for the generation of initial cyclic organic species by oxygen-containing intermediates starting from acetaldehyde has been proposed.[79,161] After the generation of MCP and aromatics, both can undergo repeated methylation/alkylation to produce a series of polyalkyl-substituted neutral and corresponding carbenium ions analogues, which then split off light olefins through dealkylation/cracking, thus completing MCP-based cycle[109] and aromatics-based cycle[106−108] via the side-chain methylation route and/or paring route. Concurrently, aromatics also undergo alkylation to form longer-chain substituted aromatics (e.g., butylation),[157,162] followed by isomerization/rearrangement and cyclization to produce indenyl, hydroindenyl, and hydronaphthyl species,[162] which further cyclize and dehydrogenate (via HT with methanol) to yield polymethyl naphthalene. An alternative pathway involves direct rearrangement of polymethylbenzenes to produce these bicyclic species.[163,164] Similarly, through these ring extension pathways, phenanthrene and other more condensed PAHs can be further generated. Furthermore, in some 8-MR cavity-type zeolites in which cages are connected by single 8-MR (such as SAPO-34, SAPO-35, and SAPO-18; not double 8-MR such as DNL-6), PAHs confined within a single cage, including naphthalene, phenanthrene, fluorene, and pyrene, can further form biphenyl- and/or methylene-bridged multicore PAHs through HT reactions, with multiple leaps in carbon numbers and unsaturation.[111,112] At this point, the dynamic evolution of the organic species process within zeolite confined space terminates. Notably, at low reaction temperatures, such as 573 K, during methanol conversion over SAPO-34, PAHs do not form; instead, adamantanes[165,166] generate as inactive coke species, and they can decompose at high temperatures, partially restoring catalyst activity (the startup methodology derived from this discovery has been applied to DMTO plants). Analogous to the autocatalytic hypercycle network described in Section 2.1, which is modulated by zeolite confined space, acidity and reaction conditions (particularly temperature), the end point of the evolution of organic species is also multifactor-determined,[31,111,131,132,134,135,165−168] likely due to the thermodynamic stability of the terminal structures of C−C bond assemblies (i.e., the largest inactive coke species) under specific zeolite (structure, dimension, and confined microenvironment) and reaction temperature conditions. Additionally, on the outer surface of the zeolite, the external coke (e.g., graphitic coke; dominant in ZSM-5[31,137−142] and to a small extent in SAPO-34[111]) can form/grow noncatalytically via thermal reactions,[142] a mechanism likely relevant to coke formation/growth in any high-temperature processes,[169,170] such as FCC or thermal cracking.[31]

Almost all chemistries in zeolite acid catalysis are involved in the dynamic evolution of organic species and the C−C bond assembly process in methanol conversion (Figure 3), including methylation, alkylation, oligomerization, cracking, dealkylation, HT, cyclization, ring expansion, ring contraction, aromatization, protonation, deprotonation, Prins reaction, Diels−Alder reaction, carbonylation, and decarbonylation, among others, and it is nearly impossible to extract any individual reaction from such a complex network. The increase in carbon number is primarily driven by methylation and alkylation reactions, utilizing C1 species (methanol, dimethyl ether (DME), SMS, formaldehyde) and light olefins as methylation and alkylation reagents, respectively. Notably, the increase in unsaturation of organic species is mainly driven by HT reactions, in which hydride transfers from the H-donor (such as methanol, cyclic or chain alkane or alkene, and aromatics) to the H-acceptor (frequently methanol and alkenes), resulting in the more H-deficient species (HCHO, polyenes, aromatics and PAHs), along with the H-saturated (cyclo)alkanes species (including methane), respectively.[9−11,70,74,141,155,156,171−180] The HT

https://doi.org/10.1021/jacs.4c12145
J. Am. Chem. Soc. 2025, 147, 11585−11607

pathways in zeolite-catalyzed methanol conversion include two categories:[154] reactant-induced HT (RIHT) and product-induced HT (PIHT) pathways, using reactant (methanol and DME) and products (olefins, i.e. conventional olefin-induced HT (OIHT)[9,11,155]) as hydrogen acceptors to produce methane, alkanes and corresponding H-deficient species. The RIHT and PIHT pathways respectively drive the product- and reactant-induced deactivation processes.[8,154] Additionally, RIHT also includes pathways where reactants (methanol and DME) serve as hydrogen donors,[11,141,155,156] leading to the formation of formaldehyde, which subsequently triggers a series of HCHO-mediated reactions and deactivation process.[10,155,156,171−174] The role of HCHO in the reaction network encompasses its further involvement in the Prins reaction with olefins, leading to the formation of polyenes, and in the alkylation reaction with aromatics, resulting in products mediated by benzyl carbenium ions.[10,142,155,156,171−174] By engaging in these reactions, HCHO assists in the formation of active HCP species in the initial stage and in the generation of light PAHs and cross-linking of PAHs[112,142] during the deactivation stage, ultimately accelerating both the initiation and deactivation of reaction.[10,38,141,154−156,171−174,181−183] For this reason, HCHO-related issues in methanol conversion has gained significant attention in recent years, including its quantification, generation, role and regulation.[10,38,154−156,171−174,180−186] The quantification and assessment of *in situ* generated HCHO are crucial and challenging for this topic. Notably, *in situ* generated HCHO differs in concentration and diffusion from cofeeding HCHO, which does not fully capture *in situ* behavior or guarantee alignment with realistic and rational conditions. Moreover, a comprehensive view of the entire complex reaction network (as shown in Figure 3) is essential, given that numerous pathways, particularly, the OIHT, exert effects on MTO (reaction deactivation and initiation) akin to HCHO, and it is challenging to quantitatively discern their respective impacts.

Consequently, throughout the full dynamic evolution of the organic species process within the confined acid microenvironment of zeolites, HT reactions play a decisive role. HT reactions not only drive the generation of unsaturated active intermediates, which are essential for constructing hypercycle network for methanol conversion, but also propel their evolution into inactive PAHs species, including the cross-linked cage-passing multicore aromatic, which thus significantly contributes to the dynamic evolution of autocatalytic network from initiating to decaying.[154] Arising from differences in local chemical potential[11,156,187] at the active sites, HT reactions also exhibit dynamic evolution.[154] When the chemical potential of reactant (methanol) is relatively high during the initial and deactivation stages with partial conversion, RIHT reactions are predominant, correlating with the experimental observation of higher levels of HCHO and methane.[154] While, PIHT reactions dominate at high-efficient stage,[154,155] when the chemical potential of alkenes and zeolite surface species is very high, as methanol is fully converted to olefins via the hypercycle network, leading to lower methane levels and almost no HCHO being detected.[154,182] Comprehensively, dynamically evolving HT reactions are pivotal to the "Hidden line" of MTO, by directing the formation of active HCP species and their evolution into inactive coke species, underpinning the origin of the dynamic nature of MTO.

The above uncovered mechanism provides a fundamental understanding for mitigating catalyst deactivation. Strategies to circumvent deactivation could be conceptually achieved by mitigating coking process induced by reactants and/or products, which can be realized by inhibiting the RIHT and PIHT reactions through minimizing their local chemical potential[11,156,187] via various strategies.[154] Crucially, the local chemical potential is intimately linked to the molecules' inherent chemical properties and, separately, to their diffusion or transport properties (detailed in Section 2.3). Methanol possesses a stronger HT capability relative to DME[154,172−174] and behaves both as a hydrogen acceptor (which produces methane and H-poor species directly promoting coking process) and donor (which produces HCHO, inducing HCHO-mediated deactivation process), enabling the reactant-induced deactivation pathway critical for the MTO reaction.[8,154] In contrast, the catalyst deactivation in the DTO (DME-to-olefins) reaction is mainly caused by product-induced deactivation process, presenting the relatively homogeneous and moderate deactivation characteristics.[113,154] Accordingly, the suppression of RIHT reactions can be directly achieved by minimizing methanol chemical potential (and thus of HCHO) via strategies such as replacing methanol with DME,[154,156,172−174] decreasing methanol pressure,[188,189] diluting methanol,[188,189] cofeeding alkenes,[11] back-mixing products,[11,141] for which it inhibits the methanol being involved HT reactions, especially including the generation of HCHO. Furthermore, HCHO chemical potential can be directly reduced by scavenging generated HCHO, and several approaches have been reported, such as: adding rare-earth oxides to decompose HCHO into CO and H_2;[184,190] water cofeeding, which can eliminate slight amounts of HCHO;[154] H_2 cofeeding, where hydrogenation of HCHO is not conspicuous in MTO processes with high-pressure H_2 cofeeding.[154] Another strategy is to suppress PIHT reactions by reducing the chemical potential of alkenes, which can be achieved via the introducing cofed water to fulfill the competitive adsorption with alkenes[145,191−193] and hydrogenation of alkenes, dienes and aromatics by cofeed high-pressure H_2.[194−196] Importantly, our recent work found that cofeeding high-pressure H_2 with DME (instead of methanol)[154] capacitates the modulation of dynamic reaction network to a more moderate autocatalysis evolution with depressed HT reaction, which was endowed by the weak HT ability and frustrated mass transfer (arousing the low local chemical potential of the reactant)[113] of DME and high-pressure H_2 effect.

Another strategy is modulating coke spatial location, which is crucial and likely more important[31] than coke amount for catalyst deactivation, but also reaction performances. Nonuniform spatial distribution of coke at the rim of SAPO-34 zeolite crystals[113,120,138,145−147,150] is commonly observed, attributed to the higher acid density in the near-surface zone,[138,147,197,198] and further is elucidated by the dynamic cross-talk mechanism of the diffusion-reaction-catalyst[113] (detailed in Section 2.3). Synthesizing zeolites with uniformly distributed acidic sites could therefore mitigate this issue. Additionally, various strategies can affect the cross-talk processes, to modulating coke spatial location to achieve a relatively uniform distribution, thereby enhancing crystal utilization and mitigating deactivation, including utilizing the different diffusive properties of reactants such as DME[113] and ethanol;[150] employing the precoking strategy;[132−135] leveraging the

https://doi.org/10.1021/jacs.4c12145
J. Am. Chem. Soc. 2025, 147, 11585−11607

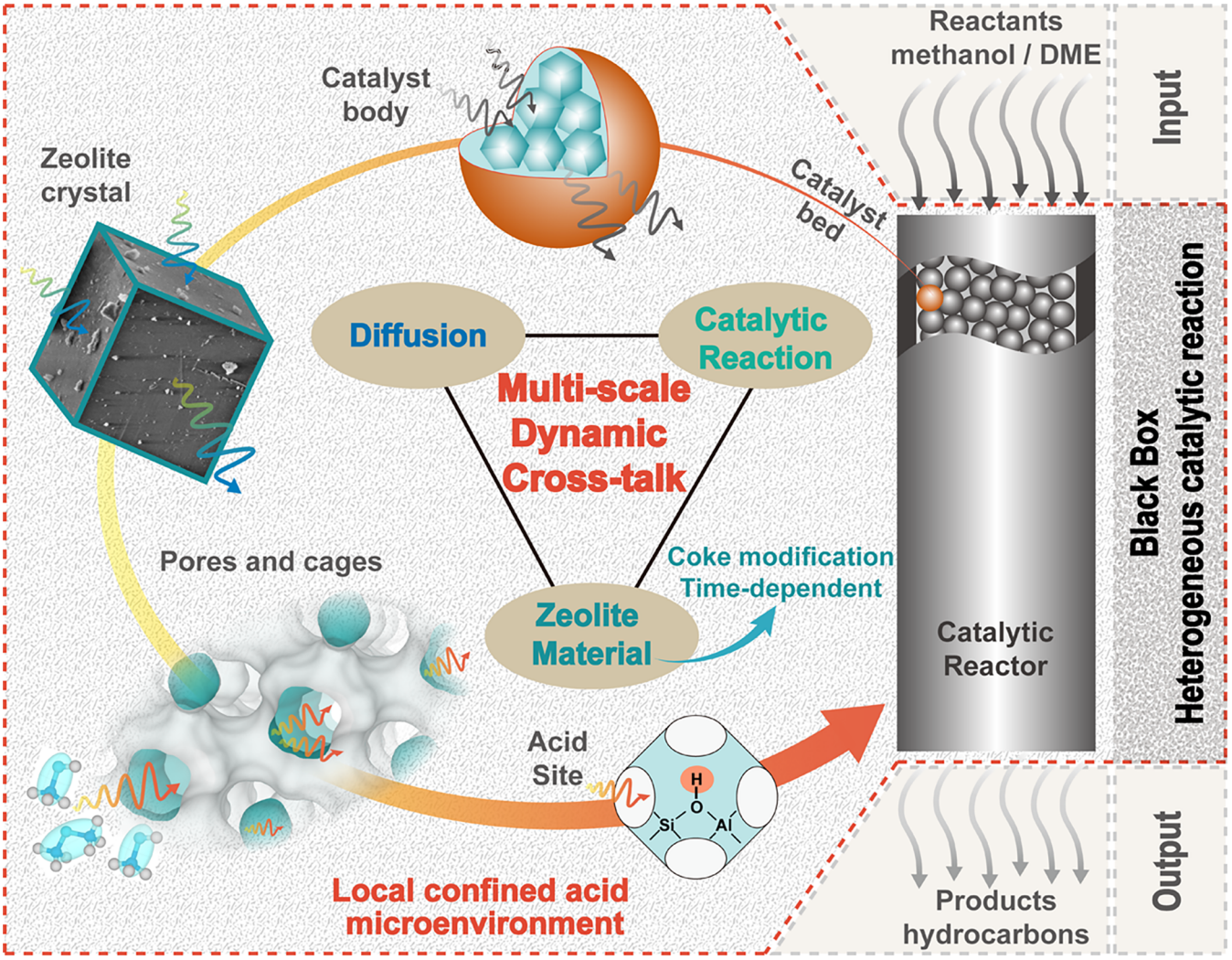

Figure 4. Multiscale dynamic cross-talk of diffusion-reaction-catalyst (coke modification) in MTO and DTO reactions over SAPO-34 across from the scale of catalytic reactor/catalyst bed (mm to m) to shaped catalyst body (μm to mm), catalyst grain/crystal (nm to μm), and active site (Å to nm). The MTO multiscale heterogeneous catalysis system is illustrated in a counterclockwise gradational magnification from the reactor to active sites: the cross-talk of diffusion−reaction−material at microscale active sites within the CHA cavity—local confined acid microenvironment—triggers multiscale cross-talk behaviors, progressively influencing the catalytic process and ultimately determining the ensemble-averaged measurements in the macroscopic reactor. The processes and the Cross-Talk concept[113] elucidated in MTO presented here may provide insights applicable to broad heterogeneous catalytic systems. The concept of the figure is based on ref [113].

competitive adsorption of water;[145] and reducing crystal size of SAPO-34[120] (detailed in Section 3.3).

2.3. Dynamic Cross-Talk Mechanism of Diffusion-Reaction-Catalyst (Coke Modification) in MTO. Two prominent features of zeolites are molecular sieving and the confinement effect that enable shape selective catalysis by modulating the mass transport of reactants, intermediates, and products within molecule-sized confines. The DMTO technology, employing SAPO-34 as a catalyst characterized by large CHA cavity and small 8-MR window, which hinders the diffusion of larger hydrocarbons and selectively sieves ethene and propene as end and desired products, serves as one of the most exemplary processes for achieving efficient shape-selective catalysis using zeolites.[1,12,54,55] All three categories of shape selective catalysis,[43] reactant shape selectivity, transition-state shape selectivity, and product shape selectivity, are wholly embodied in the MTO reaction. Understanding zeolite shape-selective catalysis in MTO[199−201] is crucial for comprehending the process and controlling product selectivity. As an advancement of shape-selective catalysis and its specific manifestation in MTO, we proposed the cavity-controlled principle,[20] which systematically encompasses and illustrates cavity-controlled product distribution,[100,199,202−207] active intermediate formation,[95,96,100,204] reaction routes,[95−97,100,204,205] diffusion,[46,47,206,208−211] and catalyst deactivation.[31,111,167,168,202]

However, the zeolite-catalyzed MTO reaction is a quintessential, yet distinctly unique, heterogeneous catalytic process. In heterogeneous catalysis, including MTO, every process spans multiple scales (Figure 4), ranging typically from the lever of active site (Å to nm), catalyst grain/crystal (nm to μm), shaped catalyst body (μm to mm), to catalytic reactor/catalyst bed (mm to m), where seven classic interplay steps—including molecular diffusion, adsorption−desorption, and chemical conversion—occurring simultaneously, creating substantial gradients in concentration of reactants and products that lead to various spatiotemporal effects in all heterogeneous catalytic processes. Such inherent spatiotempo-

https://doi.org/10.1021/jacs.4c12145
J. Am. Chem. Soc. 2025, 147, 11585−11607

ral heterogeneities[34−37] result in space- and time-dependent occurrence at multiple scales. There is always a large multiplier and gap between the chemically observable events in the reactor (laboratory experiments) and those at the molecular level (calculation simulation; mechanistic description). Beyond the above commonalities, MTO is distinguished by its dynamic autocatalysis nature, which when overlapped with these multiscale heterogeneities, greatly complicates the inevitably simultaneous occurrence of diffusion and reaction.[6,212−214] Consequently, these concurrent processes further augment the complexity of the MTO reaction system and shape-selective catalysis in it, rendering this an intricate and challenging area of research while embodying a fundamental issue inherent to heterogeneous catalysis. Notably, during the diffusion and reaction of methanol on zeolites, the dynamic autocatalysis process and the ever-evolution process of organic species (detailed in Sections 2.1 and 2.2) is similar across different zeolites, and they are virtually spatially delocalized and can "randomly walk" across the channels of HZSM-5, behaving as a "fluid hydrocarbon pool".[80] However, such "walk-in-channel" behavior[80] of bulky organics cannot occur in cavity-structured zeolites such as SAPO-34. Instead, bulky organics are "imprisoned" in the cages as retained organic products due to constrained diffusion. These ever-evolving organic species associated with the complex reaction network, together with the coke deposition, dynamically modifying the catalyst material, endow the MTO catalyst materials with a dynamic evolution nature. Such time-dependent material,[113] in turn, affects and induces the dynamical diffusion and reaction (for both reactants and product molecules) process of MTO reaction proceeding within it and eventually mediates the product distribution by dynamic shape-selective catalysis. Hence, shape selective catalysis for the MTO reaction is not only simply related to the narrow 8-MR window of SAPO-34 but also intimately related to the resided organic species (which modify acidity and cavity) and the intricate reactions driven by them. In order to narrow the huge gap between the harvest from the ensemble-averaged experiments (assuming catalysts are spatially homogeneous objects) and the realistic heterogeneous catalytic process with the interplay of reaction and diffusion, it is challenging but imperative to get a full picture of the real and complex MTO process by simultaneously considering diffusion, reaction, time-dependent zeolite materials or the involved catalytic microenvironments, and their interactions at multiple scales, from macroscopic to microscopic levels (Figure 4).

To address the dynamic reaction processes and shape-selective catalysis induced by the dynamic catalytic microenvironment in real MTO systems, by integrating the multiscale and dynamic properties of reaction and catalytic materials in the MTO reaction, we proposed the multiscale dynamic cross-talk mechanism[113] of diffusion-reaction-catalyst (coke modification) to elucidate the real shape-selective catalysis with interactive behaviors and mechanisms in cavity-type zeolite catalyzed MTO reactions (Figure 4).[113] The distinct dynamic reaction processes of MTO and DTO provide an excellent opportunity to elucidate such a cross-talk mechanism and also serve as one of the most typical examples for understanding it. Even being performed in the same zeolite material and possessing very close hydrocarbon pool mechanisms,[80,113,154,173,215] the dynamical progression and coke spatiotemporal distribution of the DTO reaction (relative to MTO) is distinctly regulated by the cross-talk of diffusion-reaction-material. The multiscale cross-talk behaviors and mechanisms originate from the reactant shape-selectivity of zeolite materials in the dynamical reaction procedure of MTO and DTO.[113] Compared with methanol, mass transfer of DME is somewhat constrained over SAPO-34,[6,113,212] since its external surface permeation and intercavity hopping are hindered due to the higher energy barrier of surface permeability and intracrystalline diffusivity. The constrained mass transfer of DME elongates the reaction zone of DTO over the catalyst bed but also engenders the lower local chemical potential of the reactant, thereby generating moderate reaction kinetics and less heavier coke in the local catalyst microenvironment. Such cross-talk of diffusion—reaction—material occurring at microscale in the CHA cavity triggers the cross-talk behaviors at multiple scales:[113] (i) enabling the inner part of the catalyst crystal still accessible to quite a part of DME at the late reaction stage (as directly evidenced by the SIM measurements[113]), sustaining the turnover of DME with high capacity; and (ii) eventually leading to a relatively moderate and homogeneous reaction and deactivation mode, and higher catalyst utilization efficiency by expanding the utilization of zeolite crystals. In contrast, methanol conversion exhibits a layer-by-layer inhomogeneous reaction and deactivation mode (in line with the classic "cigar burn" model[151,216]), and meanwhile, the higher local chemical potential of methanol enables the intensified rection and deactivation localized in the outer part of the catalyst crystal, working as the main efficient zone. Correspondingly, shell deactivation usually occurs with coke deposition within the near-surface cages,[113,120,138,145−147,150] and the MTO reaction zone tends to migrate from the exterior to the inner part of the catalyst crystal with the reaction/diffusion path concurrently increased.[113,134] Such dynamical cross-talk among time-dependent material, diffusion, and reaction occurs from the catalyst-bed scale to the catalyst crystal and CHA-cavity scale, and eventually results in the spatiotemporal heterogeneity in carbonaceous species distribution at multiple scales, revealing the root of heterogeneous catalytic efficiency, shape-selective catalysis (especially reactant shape-selective catalysis), and deactivation mode.[113]

The proposed "Cross-Talk in MTO" mechanism provides a valuable framework for understanding the shape-selective catalysis and reaction-diffusion processes in broad complex zeolite catalytic systems, comprehensively considering the interplay among diffusion, reaction, coke, and zeolite catalyst materials from a dynamic and multiscale perspective. It could potentially provide a comprehensive perspective for understanding the zeolite catalytic mechanism and process, including organics spatiotemporal distribution, thereby enabling more rational approaches for regulation and control, such as (i) the mechanistic origin[134] of enhanced ethene selectivity in "precoked" SAPO-34[131−135] and silylated ZSM-5[217] materials; (ii) the different reaction patterns between MTO and ETO (ethanol-to-olefins) processes;[150] (iii) the more efficient utilization of SAPO-34 crystals when water is cofed with methanol.[145]

Based on the deep understanding derived from extensive, long-term work, the integration of active organic species with the confined acid microenvironment of zeolites not only serves as the catalysis origin of the efficient catalytic conversion of methanol but also represents a critical strategy for shape-selective catalysis. Commercialized DMTO® technology[1,2] employs the fluidized-bed continuous reaction-regeneration

https://doi.org/10.1021/jacs.4c12145
J. Am. Chem. Soc. 2025, 147, 11585−11607

technology to achieve the high reaction efficiency, but also, simultaneously, achieve the excellent product shape selectivity for light olefins by the usage of diffusion limitation endowed by carbonaceous deposition modification in SAPO-34. The third-generation DMTO (DMTO-III) technology, through the application of "precoking" techniques, achieves extended "optimal operation window"[1] and higher shape-selective catalysis. Enlighteningly, the characteristics of DTO reaction, moderately evolved reaction kinetics and depressed coke deposition, will prompt the different operation for its catalytic application, implying the possibility of realizing a long-term operation of fixed-bed DTO process.[113,154]

Zeolite catalysis not only reflects the reaction characteristics of heterogeneous catalysis but also provides enhanced, moderate or suppressed local reaction kinetics through the special catalytic microenvironment, which leads to the heterogeneity of diffusion and reaction at multiple scales, thereby realizing efficient and shape-selective catalysis.[113] For the specific dynamic reaction catalyzed by zeolite material, achieving the best spatiotemporal cooperation of material, diffusion and reaction is the most critical strategy for the optimized catalyst development and process application.[113]

3. DYNAMIC REACTION-DIFFUSION MODEL OF MTO

3.1. Reaction Kinetics of MTO. The study of the reaction kinetics is of great significance for reactor design and optimization. Generally, the kinetic models for the MTO process can be divided into two categories: the microkinetic models and the lumped kinetic models.

The microkinetic models are usually developed based on the reaction mechanism. Considering the dynamic and complex reaction mechanism, the number of elementary reaction steps in the MTO process could be very large. Manually searching the reaction network for establishing the microkinetic models, therefore, remains a nontrivial task. An interesting yet challenging approach is to automatically generate a reaction network by computer, in which the reaction rules need to be identified according to the detailed reaction mechanism. In 2001, Park and Froment first proposed that the MTO elementary reaction rules should include protonation, deprotonation, HT, methyl shift, protonated cyclopropane branching, methylation, oligomerization, β-scission, etc.[218] They developed a computer algorithm to automatically generate a microkinetic model involving 726 elementary steps and 255 species based on these reaction rules.[218] However, the MTO reaction mechanism considered in Park and Froment's work[218] is relatively simple, and the proposed reaction rules could be classified as the formation of DME, the formation of low-carbon hydrocarbons, and the formation of high-carbon olefins. It was later generally accepted that the efficient conversion of methanol over zeolites proceeds through the indirect mechanism. Following the dual-cycle rection mechanism, Kumar et al.[219] found that reaction rules for formation of aromatic HCP species[220] should be included and further developed a microkinetic model for MTO reaction over ZSM-5 zeolite. Note that the understanding of MTO mechanism is continuously deepening; the improvement of microkinetic model would never stop. Timely extracting the reaction rules from the plenty of published literature concerning the MTO reaction mechanism, and then automatically constructing the reaction networks, provides a new venue in this direction. In our recent work,[115] a Reaction Rules Topological Matrix Representation (RTMR) method to automatically identify the reaction rules directly from the published papers has been proposed. The RTMR method was tested against the reactions in the induction stage of MTO process, which shows that 21 types of reaction rules are successfully derived based on the reaction mechanisms reported in 12 articles.[115] It is expected that this strategy can extract reaction characteristics through a small amount of existing and representative reaction knowledge, which can be of interest for the automatic exploration of a heterogeneous catalytic reaction mechanism via a knowledge-driven approach.

Lumped kinetic models have long been used to simulate and optimize the MTO processes. In earlier studies, the reaction network consisted of only three or four reactions, and the olefins are regarded as a single lumped component.[85,221] In these models, the autocatalytic attribute of methanol conversion has been considered. As discussed above, for the MTO reaction over SAPO-34 zeolites, the coke deposition on the catalyst affects both the product selectivity and conversion of methanol. Therefore, the coke content on the catalyst has been regarded as a key parameter in MTO lumped kinetic models. Bos et al.[222] considered the impact of coke in their kinetic model by introducing an empirical parameter into each reaction equation to reveal the deactivation process due to increased coke deposition. Similarly, Chen et al.[223] and we[224] proposed a deactivation function for each reaction equation to account for catalyst deactivation.

Taking the dual-cycle mechanism into account, we proposed a kinetic model,[116] in which the coke on catalyst is incorporated as an intermediate species, for MTO over SAPO-34 catalyst. In establishing the proposed kinetic model, simplifications are made by treating the olefins-based cycle as virtual species S, and the aromatics-based cycle as R, where the former mainly accounts for the production of higher olefins, and the latter for that of lower olefins. Transformation from S to R is accounted for in the reaction network in the presence of methanol and olefins (as shown in Figure 5a).

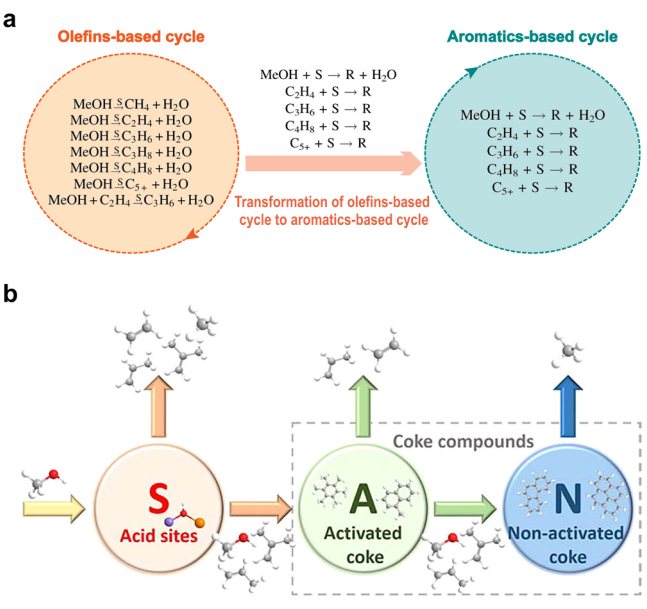

Figure 5. MTO reaction kinetics based on the dual-cycle mechanism: (a) simplified reaction network; (b) representation of coke compounds. Adapted with permission from ref [117]. Copyright 2019 Elsevier.

https://doi.org/10.1021/jacs.4c12145
J. Am. Chem. Soc. 2025, 147, 11585−11607

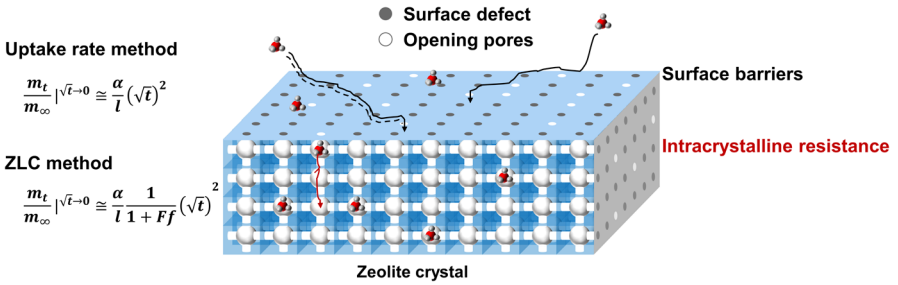

Figure 6. Schematic illustration of surface barriers for guest molecules over zeolite crystal surface and quantitative expression of surface permeability based on uptake rate[118] and ZLC[119] methods.

Meanwhile, a phenomenological deactivation model was proposed to account for the deactivation process[116]

$$\frac{d\phi}{dc_c} = -k_d\phi\left(\frac{c_c^{\max} - c_c}{c_c^{\max} - c_c^{cri}}\right)^{-n} \tag{1}$$

where ϕ (c_c) (in dimensionless) is deactivation function of catalyst. Under this assumption, the effect of the active olefins-based and aromatics-based species could be represented by ϕS and ϕR, respectively. Therefore, the reaction rate could reflect the significant decrease of ϕR when the coke content C_c approaches the critical coke content c_c^{cri}. Based on the simplified dual-cycle mechanism, the initial and highly efficient stage, as well as the deactivation process in the MTO reaction, could be quantified.

As detailed in Section 2, the evolution of HCP organic species in zeolites during the MTO reaction initially enhances the catalytic activity by forming the monocyclic and bicyclic aromatics, serving as the active coke, and eventually leads to catalyst deactivation due to the generation of tricyclic and polycyclic aromatics, referred to as the nonactive coke, which could hinder the diffusion of reactant and product molecules or block the nanopores. Such mechanisms had not been considered in MTO kinetics. Therefore, in subsequent research, we divided the coke compounds R into activated coke A and nonactive coke N (Figure 5b).[117] Thus, the empirical deactivation function described in eq 1 is unnecessary, as the transformation of A and N inherently accounts for the deactivation induced by coke deposition. In this sense, the intracrystalline diffusion as well as surface barriers can be explicitly incorporated in the kinetic model.

3.2. Diffusion of Guest Molecules in MTO over Zeolites. Diffusion is an important factor affecting the catalytic efficiency of MTO over zeolite catalysts. Recent studies have identified that the resistance of mass transfer of guest molecules in zeolites includes surface barriers as well as intracrystalline diffusion resistance.[225,226] Remi et al.[225] recorded the evolution of methanol concentration in SAPO-34 zeolites by use of interference microscopy (IFM). Their results show that for some zeolite crystals, the intracrystalline diffusion is relatively fast and the surface permeation is relatively slow, indicating that the mass transfer is dominated by surface barriers of guest molecules. For some other zeolite crystals, the surface permeation is relatively fast, and intracrystalline diffusion could be dominant. In our previous work,[226] the surface-barriers limited process was also observed using SIM.

To quantitatively describe the mass transfer in MTO, we have tried to develop measurement methods[118,119] to simultaneously obtain the surface permeability α, and intracrystalline diffusivity D. We first established a method to derive these two resistances based on the uptake rates of guest molecules in zeolites (Figure 6). From the macroscopic equations of mass transfer in zeolites, we obtained an analytical expression of surface permeability through mathematical derivation[118]

$$\frac{m_t}{m_\infty}\Big|^{\sqrt{t}\to 0} = \frac{\alpha}{l}(\sqrt{t})^2 \tag{2}$$

where m_t/m_∞ is the relative uptake loading of guest molecules, t the uptake time, l the half thickness of the plane sheet, i.e., characteristic length of the intracrystalline diffusion. The surface permeability of zeolites, according to eq 2, can be first derived from the initial relative uptake loading. The intracrystalline diffusivity D can then be calculated from the following equation:[118,227]

$$\frac{m_t}{m_\infty} = 1 - \sum_{n=1}^{\infty}\frac{2L^2}{\beta_n^2(\beta_n^2 + L^2 + L)}\cdot\exp\left(-\beta_n^2\frac{D}{l^2}t\right) \tag{3}$$

Eqs 2 and 3 can also be used for desorption processes supposing that m_t/m_∞ represents the relative release quantity of guest molecules. Using this method, we showed that the measured intracrystalline diffusion coefficients of guest molecules in zeolites do not rely on the measurement techniques and are intrinsic to the zeolite structures and independent of the crystal size and surface properties.[118]

We also developed a measurement method based on the zero-length column (ZLC).[119] In ZLC, there is a rapid flow surrounds the zeolite crystals, and the gas phase concentration is a function of time. We extended the traditional ZLC method, based on a derived theoretical expression of the desorption rate, to decouple the surface barriers and intracrystalline diffusivity from the effective diffusivity of guest molecules in nanoporous materials (Figure 6) with the following formula:[119]

$$\frac{m_t}{m_\infty}\Big|^{t\to 0} = \frac{\alpha}{l}\frac{1}{1+Ff}(\sqrt{t})^2 \tag{4}$$

$$\frac{c_t}{c_0} = \sum_{n=1}^{\infty}\frac{2H}{(\beta_n^2 + H^2 + H)}\cdot\exp\left(-\beta_n^2\frac{D}{l^2}t\right) \tag{5}$$

where c_t is the concentration of adsorbate molecules in the gas flowing out of the ZLC cell at time t, c_0 is right-hand limit of the function c_t as t approaches 0, and c_t/c_0 is the normalized concentration at the release time t. We experimentally studied the diffusion of ethane in SAPO-34 zeolite, and showed that intracrystalline diffusivity D measured by ZLC is consistent

https://doi.org/10.1021/jacs.4c12145
J. Am. Chem. Soc. 2025, 147, 11585−11607

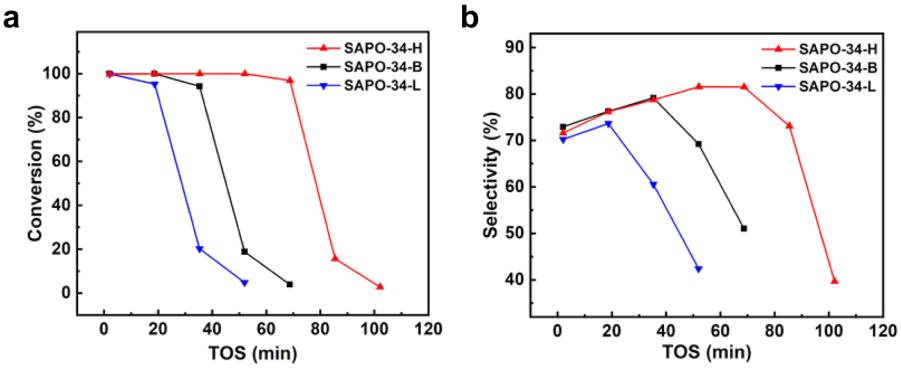

Figure 7. Methanol conversion and light olefin selectivity as a function of time on stream in the MTO reaction over SAPO-34 samples. Reprinted with permission from ref [228]. Copyright 2020 John Wiley and Sons.

with that by the PFG NMR technique.[119] In addition, we studied the diffusion of propane in SAPO-34 zeolites, and found that α and D measured by both the first uptake rate method and ZLC method agree well.[119]

We further demonstrated that the MTO reaction can be modulated by regulating surface permeability of SAPO-34 zeolites. In doing so, the surface of the SAPO-34 zeolites was modified by use of the improved chemical liquid deposition and acid etching.[228] It was shown that the reduction of surface barriers results in an obvious improvement in the mass transfer rate of methanol, thereby increasing the methanol concentration in the crystals. For olefin molecules, however, the olefin concentration inside the crystals is affected by surface barriers in a more complicated way, depending on whether the formation rate or diffusion rate is dominant. The uptake rate measurements of methanol and propane over SAPO-34 zeolites show that the reduction of surface barriers can prolong catalyst lifetime and promote light olefins selectivity (Figure 7).[228] It may imply that the reduction of surface barriers preferentially enhances the diffusion rate of olefins in the process.

3.3. Reaction-Diffusion Model of MTO. In MTO, the diffusion of guest molecules and the reaction are closely coupled. Despite the surface barriers,[228] MTO is also influenced by intracrystalline diffusion resistance. More importantly, as a dynamic and complex cross-talk process (detailed in Section 2.3), the generation and deposition of coke during the MTO process leads to the blockage of zeolite pores, substantially impeding molecular diffusion. The reaction-diffusion model provides an effective way to quantitatively understand these complex processes.

In zeolites, the change in the loading of component i with time due to reaction and diffusion is described by the following equation:

$$\frac{\partial q_i}{\partial t} = -\nabla \cdot \vec{N}_i + r_i \tag{6}$$

where q_i is the loading (concentration) of component i, t is time, $\vec{N}_i$ is molar flux vector of compound i, and r_i is reaction rate of component i. The molar flux vector $\vec{N}_i$ can be predicted by the Maxwell−Stefan diffusion theory:[117,229,230]

$$-\frac{\theta_i}{RT}\nabla\mu_i = \sum_{\substack{j=1 \\ j\neq i}}^{n} \frac{q_j\overrightarrow{N_i} - q_i\overrightarrow{N_j}}{q_i^{sat}q_j^{sat}D_{ij}} + \frac{\overrightarrow{N_i}}{q_i^{sat}D_i}(i = 1, 2, ..., n) \tag{7}$$

where μ_i is the molar chemical potential of compound i, R is the gas constant, T is the absolute temperature, q_i^{sat} is the saturated adsorption capacity of compound i, D_i is the diffusion coefficient of compound i, D_{ij} is the exchange coefficient between compound i and j, and θ_i is the fractional occupancy of compound i which is defined as $\theta_i \equiv \frac{q_i}{q^{sat}}$. The gradient of the chemical potential can be expressed in terms of the gradient of θ_i by introducing the thermodynamic correction factors Γ_{ij},[229,230]

$$\frac{\theta_i}{RT}\nabla\mu_i = \sum_{j=1}^{n}\Gamma_{ij}\nabla\theta_j,\ \Gamma_{ij} = \frac{\theta_i}{p_i}\frac{\partial p_i}{\partial\theta_j}(i = 1, 2, ..., n) \tag{8}$$

here, p_i is the pressure of gas compound i. The matrix $[\Gamma]$ can be computed following the ideal adsorbed solution theory (IAST)[131] with the experimentally measured parameters of the pure-compound adsorption isotherm. And the coefficient D_{ij} can be predicted via the interpolation of the diffusion coefficients of pure-compound from experiments.[117,230,231]

$$q_j^{sat}D_{ij} = q_i^{sat}D_{ji} = [q_j^{sat}D_{ii}]^{\frac{q_i}{q_i+q_j}}[q_i^{sat}D_{jj}]^{\frac{q_j}{q_i+q_j}} \tag{9}$$

In order to simulate the MTO process, we implemented the reaction kinetic model based on the dual-cycle mechanism, coupled with the measured diffusion coefficients of the components.[117]

Based on the reaction-diffusion model, we first compared the simulation results with the experimental data for MTO over SAPO-34 zeolites for three different zeolite sizes: 8 μm (SAPO-L), 4 μm (SAPO-M) and 1 μm (SAPO-S).[117] The results showed that reducing diffusion resistance (shortening the diffusion pathway) prolongs catalyst lifetime. For smaller crystal size, shortening the diffusion pathway of product molecules inside SAPO-34 zeolites decreases the aromatization rate from initial olefin products. At the initial and high-efficient reaction stages, the consumption rate of acid sites is relatively slow for smaller crystal sizes, due to the faster diffusion rate of product molecules. However, after the zeolite catalyst being completely deactivated, there are still about 20% of inaccessible free acid sites surrounded by aromatic compounds. The

https://doi.org/10.1021/jacs.4c12145
J. Am. Chem. Soc. 2025, 147, 11585−11607

amount of retained acid sites increases in the following order: SAPO-S < SAPO-M < SAPO-L, indicating that downsizing the SAPO-34 zeolite crystal enhances the utilization and accessibility of acid sites. This leads to the increasing total quantity of coke in SAPO-34 zeolites as the zeolite crystal size decreases.

Furthermore, the spatiotemporal evolution of carbonaceous species inside SAPO-34 zeolite crystals can also be obtained by use of SIM measurements.[120] The results showed that the distributions of HCP species (activated-coke) and coke precursors (nonactivated-coke) obtained from reaction−diffusion simulations qualitatively agree with the SIM images for SAPO-34 zeolites with different crystal sizes. For the smaller SAPO-34 zeolites, the concentration distributions of both the HCP species and coke precursors remain relatively uniform throughout the MTO process. As the crystal size increases, the spatiotemporal evolution of both HCP species and coke precursors manifests an increasingly large difference. It is also found that the formation of carbonaceous species for relatively larger SAPO-34 zeolites starts from the rim of the crystal. As the MTO proceeds, the distribution of carbonaceous species slowly expands to the interior of the crystal. After catalyst deactivation, the fluorescence intensities at the center become quite weak, indicating that carbonaceous species are rarely formed at the center of large crystals. These results clearly demonstrate that SAPO-34 zeolites with relatively smaller size favor the utilization of the active sites in MTO, which provides guidance for optimizing MTO catalyst and reaction.

4. MECHANISM AND MODEL DRIVEN MODULATION OF INDUSTRIAL PROCESS

4.1. Modeling Catalyst Coke Distribution in MTO Reactor. The reaction-diffusion mechanism and quantitative model of MTO clearly reveal how the formation of coke affects the methanol conversion as well as the formation and diffusion of light olefins, which are certainly beneficial to the optimization of industrial operation. In an industrial MTO unit, which essentially consists of a turbulent fluidized bed reactor and regenerator in the DMTO process, the coke content in the catalyst manifests a distribution because the circulation of catalyst particles between the reactor and regenerator inevitably leads to a distribution of catalyst residence time in both the reactor and regenerator. The coke distribution of catalyst particles can be mathematically quantified by a probability density function (PDF). As discussed above, for the MTO process, the coke deposited in the catalyst has an essential effect on the light olefins selectivity as well as the methanol conversion. Therefore, careful control of the catalyst coke distribution is highly desired to improve the catalytic performance of the MTO reactor.

To describe the coke distribution function of a population of catalyst particles, we derived the following governing equation based on the mass conservation:[114]

$$\frac{\partial \rho_{cat}(\vec{x}, t)p(\vec{x}, c_c, t)}{\partial t} + \nabla\cdot[\vec{v}(\vec{x}, t)\rho_{cat}(\vec{x}, t)p(\vec{x}, c_c, t)] + \frac{\partial[R(c_c)\rho_{cat}(\vec{x}, t)p(\vec{x}, c_c, t)]}{\partial c_c} = 0 \tag{10}$$

where $\rho_{cat}(\vec{x}, t)$ represents the time-dependent mass density of catalyst particles at location $\vec{x}$ and time t, $p(\vec{x}, c_c, t)$ is the coke distribution function, $\vec{v}(\vec{x}, t)$ is space velocities, $R(c_c)$ is the coke deposition rate. Here $\rho_{cat}(\vec{x}, t)$ refers to the mass density of net catalyst particles, not including the coke deposited on them. Eq 10 is a time-dependent 3D partial differential equation (PDE) for the coke distribution based on the catalyst mass density. This equation can be solved by coupling with other conservation equations, which may provide the information on velocity and density of catalyst particles. In the simulations of a catalytic process, different assumptions, such as complete mixing and plug flow, are commonly used to simplify the reactor model. The coke distribution equation, i.e., eq 10, could be also simplified based on these assumptions.[116]

By assuming the catalyst coke deposition in MTO reactor as a zero-dimensional steady-state problem, the coke distribution function can be obtained from eq 10

$$p(c_c) = \frac{1}{\tau R(c_c)} \int_{c_c^{\min}}^{c_c} p_{in}(c_c^{ini}) e^{-\int_{c_c^{ini}}^{c_c} \frac{1}{\tau R(s)} ds} dc_c^{ini} \tag{11}$$

Where τ is the average residence time of catalyst particles, $c_c^{\min}$ is the minimum coke content of inflow catalyst particles, and $p_{in}(c_c)$ is the coke distribution function of inflow catalyst particles. If the inflow catalyst particles have only a single coke content, i.e., c_c^0, which represents that $p_{in}(c_c)$ is a delta function, i.e., $p_{in}(c_c) = \delta(c_c - c_c^0)$, the above equation could be simplified as

$$p(c_c) = \frac{1}{\tau R(c_c)} e^{-\int_{c_c^0}^{c_c} \frac{1}{\tau R(s)} ds} \tag{12}$$

Based on the developed MTO kinetics,[116] the coke deposition rate can be expressed as

$$R(c_c) = k_d(c_c^{\max} - c_c) \tag{13}$$

where $c_c^{\max}$ is the maximum coke content of the catalyst particle, k_d is the deposition rate constant, which is related to the densities of methanol and olefins. Then the coke distribution function can be further simplified to the following form:

$$p(c_c) = \frac{1}{\tau k_d(c_c^{\max} - c_c)} \left(\frac{c_c^{\max} - c_c}{c_c^{\max} - c_c^0} \right)^{\frac{1}{\tau k_d} - 1} \tag{14}$$

As shown in eq 14, $\tau k_d = 1$ suggests that the coke distribution is uniform. Meanwhile, τk_d reduces eq 14 to either a monotonically decreasing function with low coke content dominating (<1), or a monotonically increasing function with the superiority of high coke content. This indicates that we can modulate the coke distribution to an appropriate reactor design by varying the parameter τk_d

For an industrial MTO reactor, however, the coke distribution function of inflow catalyst particles is usually not a delta function. In such case, the coke distribution functions of MTO reactor and regenerator can be solved iteratively.[114] We have simulated MTO reactors of different scales (laboratory pilot scale, 300t/a methanol feed rate; demonstration scale, 16 kt/a methanol feed rate; and industrial commercial scale, 1.8 MMt/a methanol feed rate), by combining the coke distribution model, MTO kinetic model, and the well-established fluidized bed reactor model.[114] All simulation results were in good agreement with the experimental data

https://doi.org/10.1021/jacs.4c12145
J. Am. Chem. Soc. 2025, 147, 11585−11607

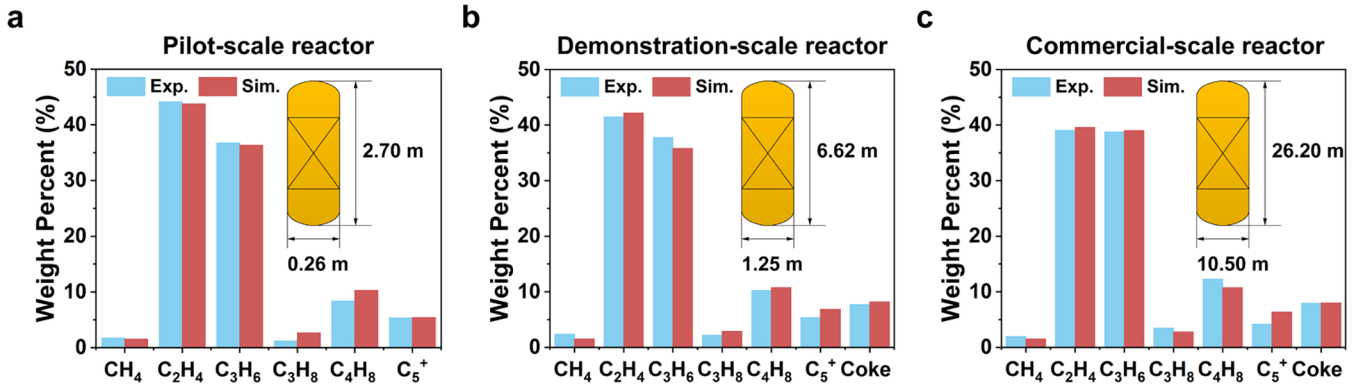

Figure 8. Simulation results of MTO reactors at different scales based on coke distribution equation and compared with experiment data. (a) Pilot-scale reactor: diameter 0.26 m, height 2.70 m; (b) Demonstration-scale reactor: diameter 1.25 m, height 6.62 m; (c) Commercial-scale reactor: diameter 10.50 m, height 26.20 m. Adapted with permission from ref [114]. Copyright 2019 John Wiley and Sons.

(Figure 8). This suggests that the coke distribution model can be potentially applied to optimize the MTO fluidized bed reactor design and operation.

4.2. Controlling of Coke Distribution in MTO Reactor.

Note that the selectivity of light olefins is closely related to the coke distribution, and it is possible to control the product yields in the MTO reactor by using the coke distribution model. A detailed analysis shows that for an MTO fluidized bed reactor-regenerator system, if the inflow catalyst particles from the regenerator to reactor have no or negligibly small coke content, the coke distribution might be dominated by the catalyst particles with light coke deposition or heavy coke deposition, depending on the coke formation rate. Meanwhile, if the coke formation rate in the fluidized bed reactor is constant, a homogeneous coke distribution of inflow catalyst particles would lead to a uniform coke distribution in the reactor. These findings could beneficially assist us in designing a novel MTO reactor with higher light olefins yields.

Furthermore, we found that the mass transfer between gas and catalyst particles only has a negligible effect on the reaction, and thus, the coke distribution dominates the product selectivity and reactant conversion in MTO.[114] This suggests that coke distribution is a potential way to scale up the MTO fluidized bed reactor.

In 2020, we proposed an efficient approach for modulating the coke distribution in an industrial DMTO reactor-regenerator system, which led to the successful development of a new generation of catalyst and design of the DMTO-III technology.[60] In DMTO-III, the methanol-to-olefins reaction is significantly enhanced by optimizing the coke distribution of catalyst particles in the reactor so that methanol can be effectively converted to ethylene and propylene with a selectivity of 85%−90% without recycling C_4^+ hydrocarbons for further cracking. More importantly, the feed rate of methanol for a DMTO-III fluidized-bed reactor can be enlarged to 3.6 MMt/a, with light olefins production of 1.35 MMt/a (Figure 9).[60] As of December 2024, the DMTO-III technology has been licensed for ten commercial units, with two already in operation.

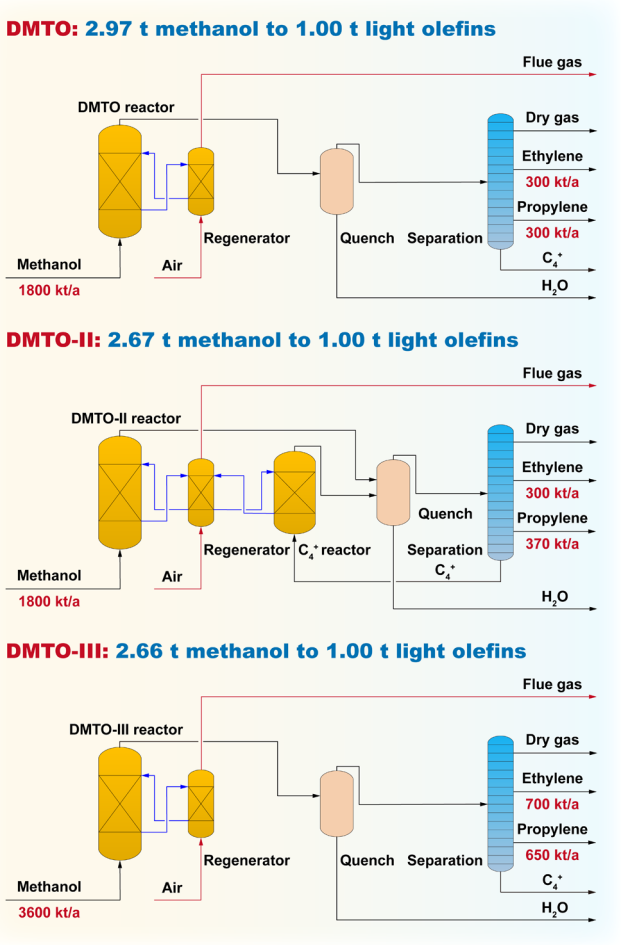

Figure 9. Simplified process diagrams for DMTO, DMTO-II and DMTO-III technologies. Adapted with permission from ref [60]; The DMTO-III data has been updated based on current industrial operational status. Available under a CC-BY 4.0 license. Copyright 2021 The Authors.

5. PERSPECTIVES AND OUTLOOK

The zeolite-catalyzed methanol conversion process, although starting from methanol, a simple C1 feedstock, is an extremely complex heterogeneous catalytic system, characterized by dynamic evolution across multiple spatial and temporal scales. The C−C bond assembly process within confined acid microenvironment of zeolite evolves from C1-feedstocks to first C−C bond, olefins, MCP, aromatics, naphthalene, PAHs and eventually cross-linked PAHs in a domino-like manner. When the methanol conversion is performed over a zeolite catalyst, light olefins can be produced with the aid of shape

https://doi.org/10.1021/jacs.4c12145
J. Am. Chem. Soc. 2025, 147, 11585−11607

selective catalysis. Simultaneously, the ever-evolving organic species within zeolite confined acid microenvironment from generation to aging, as the hidden line that guides the entire MTO dynamic autocatalysis process from the initiation, to sustaining, and to decay, in which the organic-free zeolite catalyst is transferred to a working catalyst and then to a deactivated catalyst, corresponding to the three dynamic stages of the MTO: induction, high-efficient, and deactivation. The dynamic development of the reaction network is based on the relay generation and functioning of the active centers, which evolve from acidic protons to the SMS, and then to active centers of the organic-confined zeolite microenvironment. From this point of view, highly efficient zeolite catalysis in methanol conversion extends beyond the traditional BAS catalysis category, realms into catalysis from the combination between the generated organic substances and the confined acid microenvironment of zeolite

The dynamic MTO reaction is inevitably accompanied by coke formation and deposition, which causes time-dependent variation of zeolite materials and a depressed diffusion behavior of guest molecules. These concurrent processes and their interactions further augment the complexity of the MTO reaction system but simultaneously provide the potential for achieving shape-selective catalysis. We proposed the multiscale dynamic cross-talk mechanism of diffusion-reaction-catalyst (coke modification) to provide a valuable framework for understanding the shape-selective catalysis and reaction-diffusion processes in MTO and, more broadly, in complex zeolite catalytic systems. For zeolite catalysis, especially MTO catalysis, the specific dynamic catalytic system, achieving the best spatiotemporal cooperation of the zeolite materials (with coke modification), diffusion, and reaction is the most critical strategy for the optimized catalyst development and process application.

Through the regulation of coke formation, an efficient and highly selective MTO process has been achieved, marking the realization of the new-generation technology, DMTO-III. These advancements are also elucidated by the kinetic models of reaction-diffusion. This regulation based on mechanisms and models is believed to be a valuable experience. It not only promotes the advancement of MTO but also serves as a general and potentially valuable reference for regulating a wide variety of industrially important heterogeneous catalytic processes. The understanding of the dynamic and complex MTO reaction system enriches our knowledge for zeolite catalysis and C1 chemistry.

It calls for continuous work with sustainable effort to further address the questions listed in the Introduction section in the future, aiming at a deeper understanding of the dynamic complex catalysis and the regulating of the MTO reaction. This is essential not only for finding a never deactivated "dream" catalyst for industrial MTO processes but also for setting up a widely applicable zeolite catalysis theory for this dynamic complex reaction system. Another direction worthy of high attention is the combination of artificial intelligence and data science with the complex zeolite catalysis, which will enable a more comprehensive decoupling of the intricate interactions within the complex MTO system, leading to a more rational iteration and upgrading in catalyst and process development and to further advance zeolite catalysis.

AUTHOR INFORMATION

Corresponding Authors

Zhongmin Liu − *National Engineering Research Center of Lower-Carbon Catalysis Technology, Dalian National Laboratory for Clean Energy, iChEM (Collaborative Innovation Center of Chemistry for Energy Materials), Dalian Institute of Chemical Physics, Chinese Academy of Sciences, Dalian 116023, P. R. China; State Key Laboratory of Catalysis, Dalian Institute of Chemical Physics, Chinese Academy of Sciences, Dalian 116023, P. R. China; University of Chinese Academy of Sciences, Beijing 100049, P. R. China;* orcid.org/0000-0002-7999-2940; Email: liuzm@dicp.ac.cn

Mao Ye − *National Engineering Research Center of Lower-Carbon Catalysis Technology, Dalian National Laboratory for Clean Energy, iChEM (Collaborative Innovation Center of Chemistry for Energy Materials), Dalian Institute of Chemical Physics, Chinese Academy of Sciences, Dalian 116023, P. R. China;* orcid.org/0000-0002-7078-2402; Email: maoye@dicp.ac.cn

Yingxu Wei − *National Engineering Research Center of Lower-Carbon Catalysis Technology, Dalian National Laboratory for Clean Energy, iChEM (Collaborative Innovation Center of Chemistry for Energy Materials), Dalian Institute of Chemical Physics, Chinese Academy of Sciences, Dalian 116023, P. R. China;* orcid.org/0000-0002-0412-1980; Email: weiyx@dicp.ac.cn

Authors

Shanfan Lin − *National Engineering Research Center of Lower-Carbon Catalysis Technology, Dalian National Laboratory for Clean Energy, iChEM (Collaborative Innovation Center of Chemistry for Energy Materials), Dalian Institute of Chemical Physics, Chinese Academy of Sciences, Dalian 116023, P. R. China*

Hua Li − *National Engineering Research Center of Lower-Carbon Catalysis Technology, Dalian National Laboratory for Clean Energy, iChEM (Collaborative Innovation Center of Chemistry for Energy Materials), Dalian Institute of Chemical Physics, Chinese Academy of Sciences, Dalian 116023, P. R. China*

Peng Tian − *National Engineering Research Center of Lower-Carbon Catalysis Technology, Dalian National Laboratory for Clean Energy, iChEM (Collaborative Innovation Center of Chemistry for Energy Materials), Dalian Institute of Chemical Physics, Chinese Academy of Sciences, Dalian 116023, P. R. China;* orcid.org/0000-0002-8768-0154

Complete contact information is available at: https://pubs.acs.org/10.1021/jacs.4c12145

Author Contributions

$^{\perp}$S.L. and H.L. contributed equally to this work.

Notes

The authors declare no competing financial interest.

ACKNOWLEDGMENTS

This work was supported by the National Natural Science Foundation of China (Grant Nos. 22288101, 21991090, 21991092, 21991093, 21991091, 22293021, 22402190). The authors gratefully acknowledge Prof. W.J. Li and the Research Center of Energy Strategy at DICP for the help of life cycle assessment (LCA).

REFERENCES

(1) Tian, P.; Wei, Y.; Ye, M.; Liu, Z. Methanol to olefins (MTO): from fundamentals to commercialization. *ACS Catal.* **2015**, *5* (3), 1922−1938.

(2) Xu, S.; Zhi, Y.; Han, J.; Zhang, W.; Wu, X.; Sun, T.; Wei, Y.; Liu, Z. Advances in catalysis for methanol-to-olefins conversion. *Adv. Catal.* **2017**, *61*, 37−122.

(3) Stöcker, M. Methanol-to-hydrocarbons: catalytic materials and their behavior. *Microporous Mesoporous Mater.* **1999**, *29* (1), 3−48.

(4) Haw, J. F.; Song, W. G.; Marcus, D. M.; Nicholas, J. B. The mechanism of methanol to hydrocarbon catalysis. *Acc. Chem. Res.* **2003**, *36* (5), 317−326.

(5) Wang, W.; Hunger, M. Reactivity of surface alkoxy species on acidic zeolite catalysts. *Acc. Chem. Res.* **2008**, *41* (8), 895−904.

(6) Chen, D.; Moljord, K.; Holmen, A. A methanol to olefins review: diffusion, coke formation and deactivation on SAPO type catalysts. *Microporous Mesoporous Mater.* **2012**, *164*, 239−250.

(7) Olsbye, U.; Svelle, S.; Bjørgen, M.; Beato, P.; Janssens, T. V. W.; Joensen, F.; Bordiga, S.; Lillerud, K. P. Conversion of methanol to hydrocarbons: how zeolite cavity and pore size controls product selectivity. *Angew. Chem., Int. Ed.* **2012**, *51* (24), 5810−5831.

(8) Olsbye, U.; Svelle, S.; Lillerud, K. P.; Wei, Z. H.; Chen, Y. Y.; Li, J. F.; Wang, J. G.; Fan, W. B. The formation and degradation of active species during methanol conversion over protonated zeotype catalysts. *Chem. Soc. Rev.* **2015**, *44* (20), 7155−7176.

(9) Ilias, S.; Bhan, A. Mechanism of the catalytic conversion of methanol to hydrocarbons. *ACS Catal.* **2013**, *3* (1), 18−31.

(10) Hwang, A.; Bhan, A. Deactivation of zeolites and zeotypes in methanol-to-hydrocarbons catalysis: mechanisms and circumvention. *Acc. Chem. Res.* **2019**, *52* (9), 2647−2656.

(11) Sun, X.; Mueller, S.; Liu, Y.; Shi, H.; Haller, G. L.; Sanchez-Sanchez, M.; van Veen, A. C.; Lercher, J. A. On reaction pathways in the conversion of methanol to hydrocarbons on HZSM-5. *J. Catal.* **2014**, *317*, 185−197.

(12) Yarulina, I.; Chowdhury, A. D.; Meirer, F.; Weckhuysen, B. M.; Gascon, J. Recent trends and fundamental insights in the methanol-to-hydrocarbons process. *Nat. Catal.* **2018**, *1* (6), 398−411.

(13) Li, T.; Shoinkhorova, T.; Gascon, J.; Ruiz-Martínez, J. Aromatics production via methanol-mediated transformation routes. *ACS Catal.* **2021**, *11* (13), 7780−7819.

(14) Hemelsoet, K.; Van der Mynsbrugge, J.; De Wispelaere, K.; Waroquier, M.; Van Speybroeck, V. Unraveling the reaction mechanisms governing methanol-to-olefins catalysis by theory and experiment. *ChemPhysChem* **2013**, *14* (8), 1526−1545.

(15) Wang, C.; Xu, J.; Deng, F. Mechanism of methanol-to-hydrocarbon reaction over zeolites: a solid-state NMR perspective. *ChemCatChem.* **2020**, *12* (4), 965−980.

(16) Dai, W.; Yang, L.; Wu, G.; Guan, N.; Li, L. Methanol to hydrocarbons. Heterogeneous catalysis for sustainable energy. *John Wiley and Sons* **2022**, 351−389.

(17) Wang, S.; Qin, Z.; Dong, M.; Wang, J.; Fan, W. Recent progress on MTO reaction mechanisms and regulation of acid site distribution in the zeolite framework. *Chem. Catalysis* **2022**, *2* (7), 1657−1685.

(18) Lin, S. Studies on dynamical catalytic mechanism of zeolite-catalyzed methanol and dimethyl ether to hydrocarbons proces. Ph.D. Dissertation. *Dalian Institute of Chemical Physics, Chinese Academy of Sciences* **2023**, 1−213.

(19) Zhang, W.; Wei, Y.; Liu, Z. Synthesis of olefins from CH_3OH. The chemical transformations of C1 compounds. *John Wiley and Sons* **2022**, 71−126.

(20) Zhang, W.; Lin, S.; Wei, Y.; Tian, P.; Ye, M.; Liu, Z. Cavity-controlled methanol conversion over zeolite catalysts. *Natl. Sci. Rev.* **2023**, *10* (9), nwad120.

(21) Wu, X.; Wei, Y.; Liu, Z. Dynamic catalytic mechanism of the methanol-to-hydrocarbons reaction over zeolites. *Acc. Chem. Res.* **2023**, *56* (14), 2001−2014.

(22) Lin, S.; Wei, Y.; Liu, Z. Autocatalytic induction period in zeolite-catalyzed methanol conversion. *Chem. Catalysis* **2023**, *3* (5), 100597.

(23) Yang, M.; Fan, D.; Wei, Y.; Tian, P.; Liu, Z. Recent progress in methanol-to-olefins (MTO) catalysts. *Adv. Mater.* **2019**, *31* (50), 1902181.

(24) Nan, W.; Yingxu, W.; Zhongmin, L. Methanol to olefins (MTO): a condensed matter chemistry. *Prog. Chem.* **2023**, *35* (6), 839−860.

(25) Prakash, G. K. S.; Olah, G.; Goeppert, A. Beyond oil and gas: the methanol economy. *ECS Trans.* **2011**, *35* (11), 31.

(26) Olah, G. A. Towards oil independence through renewable methanol chemistry. *Angew. Chem., Int. Ed.* **2013**, *52* (1), 104−107.

(27) Shih, C. F.; Zhang, T.; Li, J.; Bai, C. Powering the future with liquid sunshine. *Joule* **2018**, *2* (10), 1925−1949.

(28) Cai, R.; Zhu, H.; Li, W.; Xiao, Y.; Liu, Z. Development path of energy science and technology under"dual carbon" goals: perspective of multi-energy system integration. *Bulletin of Chinese Academy of Sciences* **2022**, *37* (4), 502−510.

(29) Chen, W.; Yi, X.; Liu, Z.; Tang, X.; Zheng, A. Carbocation chemistry confined in zeolites: spectroscopic and theoretical characterizations. *Chem. Soc. Rev.* **2022**, *51* (11), 4337−4385.

(30) Gong, X.; Çağlayan, M.; Ye, Y.; Liu, K.; Gascon, J.; Dutta Chowdhury, A. First-generation organic reaction intermediates in zeolite chemistry and catalysis. *Chem. Rev.* **2022**, *122* (18), 14275−14345.

(31) Vogt, E. T. C.; Fu, D.; Weckhuysen, B. M. Carbon deposit analysis in catalyst deactivation, regeneration, and rejuvenation. *Angew. Chem., Int. Ed.* **2023**, *62* (29), e202300319.

(32) Weckhuysen, B. M. Preface: recent advances in the in-situ characterization of heterogeneous catalysts. *Chem. Soc. Rev.* **2010**, *39* (12), 4557−4559.

(33) Weckhuysen, B. M. Studying birth, life and death of catalytic solids with operando spectroscopy. *Natl. Sci. Rev.* **2015**, *2* (2), 147−149.

(34) Weckhuysen, B. M. Chemical imaging of spatial heterogeneities in catalytic solids at different length and time scales. *Angew. Chem., Int. Ed.* **2009**, *48* (27), 4910−4943.

(35) Buurmans, I. L. C.; Weckhuysen, B. M. Heterogeneities of individual catalyst particles in space and time as monitored by spectroscopy. *Nat. Chem.* **2012**, *4*, 873−886.

(36) Meirer, F.; Weckhuysen, B. M. Spatial and temporal exploration of heterogeneous catalysts with synchrotron radiation. *Nat. Rev. Mater.* **2018**, *3* (9), 324−340.

(37) Mitchell, S.; Michels, N.-L.; Kunze, K.; Pérez-Ramírez, J. Visualization of hierarchically structured zeolite bodies from macro to nano length scales. *Nat. Chem.* **2012**, *4* (10), 825−831.

(38) Cesarini, A.; Mitchell, S.; Zichittella, G.; Agrachev, M.; Schmid, S. P.; Jeschke, G.; Pan, Z.; Bodi, A.; Hemberger, P.; Pérez-Ramírez, J. Elucidation of radical- and oxygenate-driven paths in zeolite-catalysed conversion of methanol and methyl chloride to hydrocarbons. *Nat. Catal.* **2022**, *5* (7), 605−614.

(39) Chen, L.; Ding, X.; Wang, Z.; Xu, S.; Jiang, Q.; Dun, C.; Urban, J. J. Advances in in situ/operando techniques for catalysis research: enhancing insights and discoveries. *Surface Science and Technology* **2024**, *2* (1), 9.

(40) Lezcano-Gonzalez, I.; Campbell, E.; Hoffman, A. E. J.; Bocus, M.; Sazanovich, I. V.; Towrie, M.; Agote-Aran, M.; Gibson, E. K.; Greenaway, A.; De Wispelaere, K.; Van Speybroeck, V.; Beale, A. M. Insight into the effects of confined hydrocarbon species on the lifetime of methanol conversion catalysts. *Nat. Mater.* **2020**, *19* (10), 1081−1087.

(41) Wang, W.; Xu, J.; Deng, F. Recent advances in solid-state NMR of zeolite catalysts. *Natl. Sci. Rev.* **2022**, *9* (9), nwac155.

(42) Niu, J.; Xu, S.; Wei, Y.; Liu, Z. Applications of in-situ solid-state nuclear magnetic resonance in methanol to olefins reaction. *Science China Chemistry* **2025**, *68* (1), 134−151.

(43) Smit, B.; Maesen, T. L. M. Towards a molecular understanding of shape selectivity. *Nature* **2008**, *451* (7179), 671−678.

(44) Smit, B.; Maesen, T. L. M. Molecular simulations of zeolites: adsorption, diffusion, and shape selectivity. *Chem. Rev.* **2008**, *108* (10), 4125−4184.

https://doi.org/10.1021/jacs.4c12145
J. Am. Chem. Soc. 2025, 147, 11585−11607

(45) Kärger, J.; Ruthven, D. M.; Theodorou, D. N. *Diffusion in Nanoporous Naterials*; Wiley-VCH: Weinheim, 2012.
(46) Gao, S.; Liu, Z.; Xu, S.; Zheng, A.; Wu, P.; Li, B.; Yuan, X.; Wei, Y.; Liu, Z. Cavity-controlled diffusion in 8-membered ring molecular sieve catalysts for shape selective strategy. *J. Catal.* **2019**, *377*, 51−62.
(47) Cnudde, P.; Demuynck, R.; Vandenbrande, S.; Waroquier, M.; Sastre, G.; Speybroeck, V. V. Light olefin diffusion during the MTO process on H-SAPO-34: a complex interplay of molecular factors. *J. Am. Chem. Soc.* **2020**, *142* (13), 6007−6017.
(48) Guisnet, M.; Costa, L.; Ribeiro, F. R. Prevention of zeolite deactivation by coking. *J. Mol. Catal. A: Chem.* **2009**, *305* (1), 69−83.
(49) Liu, X.; Wang, C.; Zhou, J.; Liu, C.; Liu, Z.; Shi, J.; Wang, Y.; Teng, J.; Xie, Z. Molecular transport in zeolite catalysts: depicting an integrated picture from macroscopic to microscopic scales. *Chem. Soc. Rev.* **2022**, *51* (19), 8174−8200.
(50) Lok, B. M.; Messina, C. A.; Patton, R. L.; Gajek, R. T.; Cannan, T. R.; Flanigen, E. M. Silicoaluminophosphate molecular sieves: another new class of microporous crystalline inorganic solids. *J. Am. Chem. Soc.* **1984**, *106* (20), 6092−6093.
(51) Li, H.; Liang, J.; Wang, R.; Liu, Z.; Zhao, S. Synthesis of Silicoaluminophosphate Zeolite SAPO-34. *Petrochem. Technol.* **1987**, *16*, 340−346.
(52) Liu, Z.; Liang, J. Methanol to olefin conversion catalysts. *Curr. Opin. Solid State Mater. Sci.* **1999**, *4* (1), 80−84.
(53) Choi, M.; Na, K.; Kim, J.; Sakamoto, Y.; Terasaki, O.; Ryoo, R. Stable single-unit-cell nanosheets of zeolite MFI as active and long-lived catalysts. *Nature* **2009**, *461* (7261), 246−249.
(54) Sun, Q.; Xie, Z.; Yu, J. The state-of-the-art synthetic strategies for SAPO-34 zeolite catalysts in methanol-to-olefin conversion. *Natl. Sci. Rev.* **2018**, *5* (4), 542−558.
(55) Dusselier, M.; Davis, M. E. Small-pore zeolites: synthesis and catalysis. *Chem. Rev.* **2018**, *118* (11), 5265−5329.
(56) Li, C.; Paris, C.; Martínez-Triguero, J.; Boronat, M.; Moliner, M.; Corma, A. Synthesis of reaction adapted zeolites as methanol-to-olefins catalysts with mimics of reaction intermediates as organic structure directing agents. *Nat. Catal.* **2018**, *1* (7), 547−554.
(57) Dai, H.; Shen, Y.; Yang, T.; Lee, C.; Fu, D.; Agarwal, A.; Le, T. T.; Tsapatsis, M.; Palmer, J. C.; Weckhuysen, B. M.; Dauenhauer, P. J.; Zou, X.; Rimer, J. D. Finned zeolite catalysts. *Nat. Mater.* **2020**, *19* (10), 1074−1080.
(58) Le, T. T.; Qin, W.; Agarwal, A.; Nikolopoulos, N.; Fu, D.; Patton, M. D.; Weiland, C.; Bare, S. R.; Palmer, J. C.; Weckhuysen, B. M.; Rimer, J. D. Elemental zoning enhances mass transport in zeolite catalysts for methanol to hydrocarbons. *Nat. Catal.* **2023**, *6* (3), 254−265.
(59) Wang, Y.; Tong, C.; Liu, Q.; Han, R.; Liu, C. Intergrowth zeolites, synthesis, characterization, and catalysis. *Chem. Rev.* **2023**, *123* (19), 11664−11721.
(60) Ye, M.; Tian, P.; Liu, Z. DMTO: a sustainable methanol-to-olefins technology. *Engineering* **2021**, *7* (1), 17−21.
(61) Ye, M.; Li, H.; Zhao, Y.; Zhang, T.; Liu, Z. MTO processes development: the key of mesoscale studies. *Academic Press* **2015**, *47*, 279−335.
(62) Vora, B. V.; Marker, T. L.; Barger, P. T.; Nilsen, H. R.; Kvisle, S.; Fuglerud, T. Economic route for natural gas conversion to ethylene and propylene. *Elsevier* **1997**, *107*, 87−98.
(63) Keil, F. J. Methanol-to-hydrocarbons: process technology. *Microporous Mesoporous Mater.* **1999**, *29* (1), 49−66.
(64) Chen, J. Q.; Bozzano, A.; Glover, B.; Fuglerud, T.; Kvisle, S. Recent advancements in ethylene and propylene production using the UOP/Hydro MTO process. *Catal. Today* **2005**, *106* (1), 103−107.
(65) Koempel, H.; Liebner, W. Lurgi's methanol to propylene (MTP®) report on a successful commercialisation. *Elsevier* **2007**, *167*, 261−267.
(66) Cordero-Lanzac, T.; Gayubo, A. G.; Aguayo, A. T.; Bilbao, J. The MTO and DTO processes as greener alternatives to produce olefins: A review of kinetic models and reactor design. *Chem. Eng. J.* **2024**, *494*, 152906.
(67) Chang, C. D.; Silvestri, A. J. The conversion of methanol and other O-compounds to hydrocarbons over zeolite catalysts. *J. Catal.* **1977**, *47* (2), 249−259.
(68) Li, J.; Wei, Z.; Chen, Y.; Jing, B.; He, Y.; Dong, M.; Jiao, H.; Li, X.; Qin, Z.; Wang, J.; Fan, W. A route to form initial hydrocarbon pool species in methanol conversion to olefins over zeolites. *J. Catal.* **2014**, *317*, 277−283.
(69) Comas-Vives, A.; Valla, M.; Copéret, C.; Sautet, P. Cooperativity between Al sites promotes hydrogen transfer and carbon-carbon bond formation upon dimethyl ether activation on alumina. *ACS Cent. Sci.* **2015**, *1* (6), 313−319.
(70) Liu, Y.; Müller, S.; Berger, D.; Jelic, J.; Reuter, K.; Tonigold, M.; Sanchez-Sanchez, M.; Lercher, J. A. Formation mechanism of the first carbon-carbon bond and the first olefin in the methanol conversion into hydrocarbons. *Angew. Chem., Int. Ed.* **2016**, *55* (19), 5723−5726.
(71) Chowdhury, A. D.; Houben, K.; Whiting, G. T.; Mokhtar, M.; Asiri, A. M.; Al-Thabaiti, S. A.; Basahel, S. N.; Baldus, M.; Weckhuysen, B. M. Initial carbon-carbon bond formation during the early stages of the methanol-to-olefin process proven by zeolite-trapped acetate and methyl acetate. *Angew. Chem., Int. Ed.* **2016**, *55* (51), 15840−15845.
(72) Peng, C.; Wang, H.; Hu, P. Theoretical insights into how the first C-C bond forms in the methanol-to-olefin process catalysed by HSAPO-34. *Phys. Chem. Chem. Phys.* **2016**, *18* (21), 14495−14502.
(73) Wu, X.; Xu, S.; Zhang, W.; Huang, J.; Li, J.; Yu, B.; Wei, Y.; Liu, Z. Direct mechanism of the first carbon-carbon bond formation in the methanol-to-hydrocarbons process. *Angew. Chem., Int. Ed.* **2017**, *56* (31), 9039−9043.
(74) Plessow, P. N.; Studt, F. Unraveling the mechanism of the initiation reaction of the methanol to olefins process using ab initio and DFT calculations. *ACS Catal.* **2017**, *7* (11), 7987−7994.
(75) Chu, Y.; Yi, X.; Li, C.; Sun, X.; Zheng, A. Brønsted/Lewis acid sites synergistically promote the initial C-C bond formation in the MTO reaction. *Chem. Sci.* **2018**, *9*, 6470−6479.
(76) Wang, C.; Chu, Y.; Xu, J.; Wang, Q.; Qi, G.; Gao, P.; Zhou, X.; Deng, F. Extra-framework aluminum-assisted initial C-C bond formation in methanol-to-olefins conversion on zeolite H-ZSM-5. *Angew. Chem., Int. Ed.* **2018**, *57* (32), 10197−10201.
(77) Wu, X.; Xu, S.; Wei, Y.; Zhang, W.; Huang, J.; Xu, S.; He, Y.; Lin, S.; Sun, T.; Liu, Z. Evolution of C-C bond formation in the methanol-to-olefins process: from direct coupling to autocatalysis. *ACS Catal.* **2018**, *8* (8), 7356−7361.
(78) Plessow, P. N.; Smith, A.; Tischer, S.; Studt, F. Identification of the reaction sequence of the MTO initiation mechanism using ab initio-based kinetics. *J. Am. Chem. Soc.* **2019**, *141* (14), 5908−5915.
(79) Yang, L.; Yan, T.; Wang, C.; Dai, W.; Wu, G.; Hunger, M.; Fan, W.; Xie, Z.; Guan, N.; Li, L. Role of acetaldehyde in the roadmap from initial carbon-carbon bonds to hydrocarbons during methanol conversion. *ACS Catal.* **2019**, *9* (7), 6491−6501.
(80) Lin, S.; Zhi, Y.; Chen, W.; Li, H.; Zhang, W.; Lou, C.; Wu, X.; Zeng, S.; Xu, S.; Xiao, J.; Zheng, A.; Wei, Y.; Liu, Z. Molecular routes of dynamic autocatalysis for methanol-to-hydrocarbons reaction. *J. Am. Chem. Soc.* **2021**, *143* (31), 12038−12052.
(81) Sun, T.; Chen, W.; Xu, S.; Zheng, A.; Wu, X.; Zeng, S.; Wang, N.; Meng, X.; Wei, Y.; Liu, Z. The first carbon-carbon bond formation mechanism in methanol-to-hydrocarbons process over chabazite zeolite. *Chem.* **2021**, *7* (9), 2415−2428.
(82) Wu, X.; Chen, W.; Xu, S.; Lin, S.; Sun, T.; Zheng, A.; Wei, Y.; Liu, Z. Dynamic activation of C1 molecules evoked by zeolite catalysis. *ACS Cent. Sci.* **2021**, *7* (4), 681−687.
(83) Minova, I. B.; Bühl, M.; Matam, S. K.; Catlow, C. R. A.; Frogley, M. D.; Cinque, G.; Wright, P. A.; Howe, R. F. Carbene-like reactivity of methoxy groups in a single crystal SAPO-34 MTO catalyst. *Catal. Sci. Technol.* **2022**, *12* (7), 2289−2305.
(84) Wu, X.; Zhang, Z.; Pan, Z.; Zhou, X.; Bodi, A.; Hemberger, P. Ketenes in the induction of the methanol-to-olefins process. *Angew. Chem., Int. Ed.* **2022**, *61* (41), e202207777.

(85) Chen, N. Y.; Reagan, W. J. Evidence of autocatalysis in methanol to hydrocarbon reactions over zeolite catalysts. *J. Catal.* **1979**, *59* (1), 123−129.
(86) Dessau, R. M.; LaPierre, R. B. On the mechanism of methanol conversion to hydrocarbons over HZSM-5. *J. Catal.* **1982**, *78* (1), 136−141.
(87) Dessau, R. M. On the H-ZSM-5 catalyzed formation of ethylene from methanol or higher olefins. *J. Catal.* **1986**, *99* (1), 111−116.
(88) Mole, T.; Whiteside, J. A.; Seddon, D. Aromatic co-catalysis of methanol conversion over zeolite catalysts. *J. Catal.* **1983**, *82* (2), 261−266.
(89) Mole, T.; Bett, G.; Seddon, D. Conversion of methanol to hydrocarbons over ZSM-5 zeolite: an examination of the role of aromatic hydrocarbons using 13carbon- and deuterium-labeled feeds. *J. Catal.* **1983**, *84* (2), 435−445.
(90) Dahl, I. M.; Kolboe, S. On the reaction mechanism for propene formation in the MTO reaction over SAPO-34. *Catal. Lett.* **1993**, *20* (3), 329−336.
(91) Dahl, I. M.; Kolboe, S. On the reaction mechanism for hydrocarbon formation from methanol over SAPO-34:1. Isotopic labeling studies of the co-reaction of ethene and methanol. *J. Catal.* **1994**, *149* (2), 458−464.
(92) Dahl, I. M.; Kolboe, S. On the reaction mechanism for hydrocarbon formation from methanol over SAPO-34:2. isotopic labeling studies of the co-reaction of propene and methanol. *J. Catal.* **1996**, *161* (1), 304−309.
(93) Goguen, P. W.; Xu, T.; Barich, D. H.; Skloss, T. W.; Song, W.; Wang, Z.; Nicholas, J. B.; Haw, J. F. Pulse-quench catalytic reactor studies reveal a carbon-pool mechanism in methanol-to-gasoline chemistry on zeolite HZSM-5. *J. Am. Chem. Soc.* **1998**, *120* (11), 2650−2651.
(94) Song, W.; Nicholas, J. B.; Haw, J. F. A persistent carbenium ion on the methanol-to-olefin catalyst HSAPO-34: acetone shows the way. *J. Phys. Chem. B* **2001**, *105* (19), 4317−4323.
(95) Li, J.; Wei, Y.; Chen, J.; Tian, P.; Su, X.; Xu, S.; Qi, Y.; Wang, Q.; Zhou, Y.; He, Y.; Liu, Z. Observation of heptamethylbenzenium cation over SAPO-type molecular sieve DNL-6 under real mto conversion conditions. *J. Am. Chem. Soc.* **2012**, *134* (2), 836−839.
(96) Xu, S.; Zheng, A.; Wei, Y.; Chen, J.; Li, J.; Chu, Y.; Zhang, M.; Wang, Q.; Zhou, Y.; Wang, J.; Deng, F.; Liu, Z. Direct observation of cyclic carbenium ions and their role in the catalytic cycle of the methanol-to-olefin reaction over chabazite zeolites. *Angew. Chem., Int. Ed.* **2013**, *52* (44), 11564−11568.
(97) Li, J.; Wei, Y.; Xu, S.; Tian, P.; Chen, J.; Liu, Z. Heptamethylbenzenium cation formation and the correlated reaction pathway during methanol-to-olefins conversion over DNL-6. *Catal. Today* **2014**, *226*, 47−51.
(98) Wang, C.; Chu, Y.; Zheng, A.; Xu, J.; Wang, Q.; Gao, P.; Qi, G.; Gong, Y.; Deng, F. New insight into the hydrocarbon-pool chemistry of the methanol-to-olefins conversion over zeolite H-ZSM-5 from GC-MS, solid-state NMR spectroscopy, and DFT calculations. *Chem. - Eur. J.* **2014**, *20* (39), 12432−12443.
(99) Dai, W.; Wang, C.; Dyballa, M.; Wu, G.; Guan, N.; Li, L.; Xie, Z.; Hunger, M. Understanding the early stages of the methanol-to-olefin conversion on H-SAPO-34. *ACS Catal.* **2015**, *5* (1), 317−326.
(100) Li, J.; Wei, Y.; Chen, J.; Xu, S.; Tian, P.; Yang, X.; Li, B.; Wang, J.; Liu, Z. Cavity controls the selectivity: insights of confinement effects on MTO reaction. *ACS Catal.* **2015**, *5* (2), 661−665.
(101) Wang, C.; Wang, Q.; Xu, J.; Qi, G.; Gao, P.; Wang, W.; Zou, Y.; Feng, N.; Liu, X.; Deng, F. Direct detection of supramolecular reaction centers in the methanol-to-olefins conversion over zeolite H-ZSM-5 by 13C-27Al solid-state NMR spectroscopy. *Angew. Chem., Int. Ed.* **2016**, *55* (7), 2507−2511.
(102) Wang, C.; Hu, M.; Chu, Y.; Zhou, X.; Wang, Q.; Qi, G.; Li, S.; Xu, J.; Deng, F. π-interactions between cyclic carbocations and aromatics cause zeolite deactivation in methanol-to-hydrocarbon conversion. *Angew. Chem., Int. Ed.* **2020**, *59* (18), 7198−7202.
(103) Zhang, W.; Zhang, M.; Xu, S.; Gao, S.; Wei, Y.; Liu, Z. Methylcyclopentenyl cations linking initial stage and highly efficient stage in methanol-to-hydrocarbon process. *ACS Catal.* **2020**, *10* (8), 4510−4516.
(104) Wang, C.; Chu, Y.; Hu, M.; Cai, W.; Wang, Q.; Qi, G.; Li, S.; Xu, J.; Deng, F. Insight into carbocation-induced noncovalent interactions in the methanol-to-olefins reaction over ZSM-5 zeolite by solid-state NMR spectroscopy. *Angew. Chem., Int. Ed.* **2021**, *60* (51), 26847−26854.
(105) Wu, Y.; Han, J.; Zhang, W.; Yu, Z.; Wang, K.; Fang, X.; Wei, Y.; Liu, Z. Combined strategies enable highly selective light olefins and para-xylene production on single catalyst bed. *J. Am. Chem. Soc.* **2024**, *146* (12), 8086−8097.
(106) Svelle, S.; Joensen, F.; Nerlov, J.; Olsbye, U.; Lillerud, K.-P.; Kolboe, S.; Bjørgen, M. Conversion of methanol into hydrocarbons over zeolite H-ZSM-5: ethene formation is mechanistically separated from the formation of higher alkenes. *J. Am. Chem. Soc.* **2006**, *128* (46), 14770−14771.
(107) Bjørgen, M.; Svelle, S.; Joensen, F.; Nerlov, J.; Kolboe, S.; Bonino, F.; Palumbo, L.; Bordiga, S.; Olsbye, U. Conversion of methanol to hydrocarbons over zeolite H-ZSM-5: on the origin of the olefinic species. *J. Catal.* **2007**, *249* (2), 195−207.
(108) Bjørgen, M.; Lillerud, K.-P.; Olsbye, U.; Svelle, S. Conversion of methanol to hydrocarbons: hints to rational catalyst design from fundamental mechanistic studies on H-ZSM-5. *Stud. Surf. Sci. Catal.* **2007**, *167*, 463−468.
(109) Zhang, W.; Zhi, Y.; Huang, J.; Wu, X.; Zeng, S.; Xu, S.; Zheng, A.; Wei, Y.; Liu, Z. Methanol to olefins reaction route based on methylcyclopentadienes as critical intermediates. *ACS Catal.* **2019**, *9* (8), 7373−7379.
(110) Zhang, W.; Xu, S.; Zhi, Y.; Wei, Y.; Liu, Z. Methylcyclopentenyl cation mediated reaction route in methanol-to-olefins reaction over H-RUB-50 with small cavity. *J. Energy Chem.* **2020**, *45*, 25−30.
(111) Wang, N.; Zhi, Y.; Wei, Y.; Zhang, W.; Liu, Z.; Huang, J.; Sun, T.; Xu, S.; Lin, S.; He, Y.; Zheng, A.; Liu, Z. Molecular elucidating of an unusual growth mechanism for polycyclic aromatic hydrocarbons in confined space. *Nat. Commun.* **2020**, *11* (1), 1079.
(112) Wang, N.; Wang, L.; Zhi, Y.; Han, J.; Zhang, C.; Wu, X.; Zhang, J.; Wang, L.; Fan, B.; Xu, S.; Zheng, Y.; Lin, S.; Wu, R.; Wei, Y.; Liu, Z. Coking and decoking chemistry for resource utilization of polycyclic aromatic hydrocarbons (PAHs) and low-carbon process. *J. Energy Chem.* **2023**, *76*, 105−116.
(113) Lin, S.; Zhi, Y.; Liu, Z.; Yuan, J.; Liu, W.; Zhang, W.; Xu, Z.; Zheng, A.; Wei, Y.; Liu, Z. Multiscale dynamical cross-talk in zeolite-catalyzed methanol and dimethyl ether conversions. *Natl. Sci. Rev.* **2022**, *9* (9), nwac151.
(114) Li, H.; Yuan, X.; Gao, M.; Ye, M.; Liu, Z. Study of catalyst coke distribution based on population balance theory: application to methanol to olefins process. *AIChE J.* **2019**, *65* (4), 1149−1161.
(115) Yu, J.; Li, H.; Ye, M.; Liu, Z. A knowledge-driven approach for automatic generation of reaction networks of methanol-to-olefins process. *Chem. Eng. Sci.* **2024**, *284*, 119461.
(116) Yuan, X.; Li, H.; Ye, M.; Liu, Z. Kinetic modeling of methanol to olefins process over SAPO-34 catalyst based on the dual-cycle reaction mechanism. *AIChE J.* **2019**, *65* (2), 662−674.
(117) Gao, M.; Li, H.; Yang, M.; Zhou, J.; Yuan, X.; Tian, P.; Ye, M.; Liu, Z. A modeling study on reaction and diffusion in MTO process over SAPO-34 zeolites. *Chem. Eng. J.* **2019**, *377*, 119668.
(118) Gao, M.; Li, H.; Yang, M.; Gao, S.; Wu, P.; Tian, P.; Xu, S.; Ye, M.; Liu, Z. Direct quantification of surface barriers for mass transfer in nanoporous crystalline materials. *Commun. Chem.* **2019**, *2* (1), 43.
(119) Xie, Y.; Li, H.; Lou, C.; Ye, M.; Liu, Z. Quantifying molecular surface barriers and intracrystalline diffusion in nanoporous materials by zero-length column. *AIChE J.* **2023**, *69* (10), e18159.
(120) Gao, M.; Li, H.; Liu, W.; Xu, Z.; Peng, S.; Yang, M.; Ye, M.; Liu, Z. Imaging spatiotemporal evolution of molecules and active sites

in zeolite catalyst during methanol-to-olefins reaction. *Nat. Commun.* **2020**, *11* (1), 3641.
(121) Lesthaeghe, D.; Van Speybroeck, V.; Marin, G. B.; Waroquier, M. Understanding the failure of direct C-C coupling in the zeolite-catalyzed methanol-to-olefin process. *Angew. Chem., Int. Ed.* **2006**, *45* (11), 1714−1719.
(122) Zhang, M.; Xu, S.; Wei, Y.; Li, J.; Wang, J.; Zhang, W.; Gao, S.; Liu, Z. Changing the balance of the MTO reaction dual-cycle mechanism: reactions over ZSM-5 with varying contact times. *Chin. J. Catal.* **2016**, *37* (8), 1413−1422.
(123) Jogunola, O.; Salmi, T.; Eränen, K.; Wärnå, J.; Mikkola, J. P. Rates and equilibria of ester hydrolysis: combination of slow and rapid reactions. *Chem. Eng. Process.* **2011**, *50* (7), 665−674.
(124) Luisi, P. L. The emergence of life: from chemical origins to synthetic biology. Cambridge University Press 2006.
(125) Küchler, A.; Yoshimoto, M.; Luginbühl, S.; Mavelli, F.; Walde, P. Enzymatic reactions in confined environments. *Nat. Nanotechnol.* **2016**, *11* (5), 409−420.
(126) Gounder, R.; Iglesia, E. The catalytic diversity of zeolites: confinement and solvation effects within voids of molecular dimensions. *Chem. Commun.* **2013**, *49* (34), 3491−3509.
(127) Fu, Q.; Bao, X. Confined microenvironment for catalysis control. *Nat. Catal.* **2019**, *2* (10), 834−836.
(128) Qi, L.; Wei, Y.; Xu, L.; Liu, Z. Reaction behaviors and kinetics during induction period of methanol conversion on HZSM-5 zeolite. *ACS Catal.* **2015**, *5* (7), 3973−3982.
(129) Brogaard, R. Y.; Henry, R.; Schuurman, Y.; Medford, A. J.; Moses, P. G.; Beato, P.; Svelle, S.; Nørskov, J. K.; Olsbye, U. Methanol-to-hydrocarbons conversion: the alkene methylation pathway. *J. Catal.* **2014**, *314*, 159−169.
(130) Bissette, A. J.; Fletcher, S. P. Mechanisms of autocatalysis. *Angew. Chem., Int. Ed.* **2013**, *52* (49), 12800−12826.
(131) Song, W.; Fu, H.; Haw, J. F. Selective synthesis of methylnaphthalenes in HSAPO-34 cages and their function as reaction centers in methanol-to-olefin catalysis. *J. Phys. Chem. B* **2001**, *105* (51), 12839−12843.
(132) Zhou, J.; Gao, M.; Zhang, J.; Liu, W.; Zhang, T.; Li, H.; Xu, Z.; Ye, M.; Liu, Z. Directed transforming of coke to active intermediates in methanol-to-olefins catalyst to boost light olefins selectivity. *Nat. Commun.* **2021**, *12* (1), 17.
(133) Zhang, C.; Wu, X.; Zhang, Y.; Zhang, W.; Lin, S.; Lou, C.; Xu, S.; He, D.; Wang, L.; Wei, Y.; Liu, Z. Water-assisted shape-selective production of ethene in methanol-to-olefins reaction on SAPO-34. *Chem. Catalysis* **2024**, *4*, 101025.
(134) Zhou, J.; Zhi, Y.; Zhang, J.; Liu, Z.; Zhang, T.; He, Y.; Zheng, A.; Ye, M.; Wei, Y.; Liu, Z. Presituated "coke"-determined mechanistic route for ethene formation in the methanol-to-olefins process on SAPO-34 catalyst. *J. Catal.* **2019**, *377*, 153−162.
(135) Wang, C.; Yang, L.; Gao, M.; Shao, X.; Dai, W.; Wu, G.; Guan, N.; Xu, Z.; Ye, M.; Li, L. Directional construction of active naphthalenic species within SAPO-34 crystals toward more efficient methanol-to-olefin conversion. *J. Am. Chem. Soc.* **2022**, *144* (46), 21408−21416.
(136) Schulz, H. "Coking" of zeolites during methanol conversion: basic reactions of the MTO-, MTP- and MTG processes. *Catal. Today* **2010**, *154* (3), 183−194.
(137) Mores, D.; Kornatowski, J.; Olsbye, U.; Weckhuysen, B. M. Coke formation during the methanol-to-olefin conversion: in situ microspectroscopy on individual H-ZSM-5 crystals with different brønsted acidity. *Chem. - Eur. J.* **2011**, *17* (10), 2874−2884.
(138) Mores, D.; Stavitski, E.; Kox, M. H. F.; Kornatowski, J.; Olsbye, U.; Weckhuysen, B. M. Space- and time-resolved in-situ spectroscopy on the coke formation in molecular sieves: methanol-to-olefin conversion over H-ZSM-5 and H-SAPO-34. *Chem. - Eur. J.* **2008**, *14* (36), 11320−11327.
(139) Wang, N.; Sun, W.; Hou, Y.; Ge, B.; Hu, L.; Nie, J.; Qian, W.; Wei, F. Crystal-plane effects of MFI zeolite in catalytic conversion of methanol to hydrocarbons. *J. Catal.* **2018**, *360*, 89−96.
(140) Fu, D.; van der Heijden, O.; Stanciakova, K.; Schmidt, J. E.; Weckhuysen, B. M. Disentangling reaction processes of zeolites within single-oriented channels. *Angew. Chem., Int. Ed.* **2020**, *59* (36), 15502−15506.
(141) Müller, S.; Liu, Y.; Vishnuvarthan, M.; Sun, X.; van Veen, A. C.; Haller, G. L.; Sanchez-Sanchez, M.; Lercher, J. A. Coke formation and deactivation pathways on H-ZSM-5 in the conversion of methanol to olefins. *J. Catal.* **2015**, *325*, 48−59.
(142) Lee, S.; Choi, M. Unveiling coke formation mechanism in MFI zeolites during methanol-to-hydrocarbons conversion. *J. Catal.* **2019**, *375*, 183−192.
(143) Wennmacher, J. T. C.; Mahmoudi, S.; Rzepka, P.; Sik Lee, S.; Gruene, T.; Paunović, V.; van Bokhoven, J. A. Electron diffraction enables the mapping of coke in ZSM-5 micropores formed during methanol-to-hydrocarbons conversion. *Angew. Chem., Int. Ed.* **2022**, *61* (29), e202205413.
(144) Rzepka, P.; Sheptyakov, D.; Wang, C.; van Bokhoven, J. A.; Paunović, V. How micropore topology influences the structure and location of coke in zeolite catalysts. *ACS Catal.* **2024**, *14* (8), 5593−5604.
(145) De Wispelaere, K.; Wondergem, C. S.; Ensing, B.; Hemelsoet, K.; Meijer, E. J.; Weckhuysen, B. M.; Van Speybroeck, V.; Ruiz-Martınez, J. Insight into the effect of water on the methanol-to-olefins conversion in H-SAPO-34 from molecular simulations and in situ microspectroscopy. *ACS Catal.* **2016**, *6* (3), 1991−2002.
(146) Qian, Q.; Ruiz-Martínez, J.; Mokhtar, M.; Asiri, A. M.; Al-Thabaiti, S. A.; Basahel, S. N.; van der Bij, H. E.; Kornatowski, J.; Weckhuysen, B. M. Single-particle spectroscopy on large SAPO-34 crystals at work: methanol-to-olefin versus ethanol-to-olefin processes. *Chem. - Eur. J.* **2013**, *19* (34), 11204−11215.
(147) Schmidt, J. E.; Peng, L.; Paioni, A. L.; Ehren, H. L.; Guo, W.; Mazumder, B.; Matthijs de Winter, D. A.; Attila, Ö.; Fu, D.; Chowdhury, A. D.; Houben, K.; Baldus, M.; Poplawsky, J. D.; Weckhuysen, B. M. Isolating clusters of light elements in molecular sieves with atom probe tomography. *J. Am. Chem. Soc.* **2018**, *140* (29), 9154−9158.
(148) Schmidt, J. E.; Poplawsky, J. D.; Mazumder, B.; Attila, Ö.; Fu, D.; de Winter, D. A. M.; Meirer, F.; Bare, S. R.; Weckhuysen, B. M. Coke formation in a zeolite crystal during the methanol-to-hydrocarbons reaction as studied with atom probe tomography. *Angew. Chem., Int. Ed.* **2016**, *55* (37), 11173−11177.
(149) Devaraj, A.; Vijayakumar, M.; Bao, J.; Guo, M. F.; Derewinski, M. A.; Xu, Z.; Gray, M. J.; Prodinger, S.; Ramasamy, K. K. Discerning the location and nature of coke deposition from surface to bulk of spent zeolite catalysts. *Sci. Rep.* **2016**, *6* (1), 37586.
(150) Qian, Q.; Ruiz-Martínez, J.; Mokhtar, M.; Asiri, A. M.; Al-Thabaiti, S. A.; Basahel, S. N.; Weckhuysen, B. M. Single-particle spectroscopy of alcohol-to-olefins over SAPO-34 at different reaction stages: crystal accessibility and hydrocarbons reactivity. *ChemCatChem.* **2014**, *6* (3), 772−783.
(151) Haw, J. F.; Marcus, D. M. Well-defined (supra)molecular structures in zeolite methanol-to-olefin catalysis. *Top. Catal.* **2005**, *34* (1), 41−48.
(152) Márquez, F.; García, H.; Palomares, E.; Fernández, L.; Corma, A. Spectroscopic evidence in support of the molecular orbital confinement concept: case of anthracene incorporated in zeolites. *J. Am. Chem. Soc.* **2000**, *122* (27), 6520−6521.
(153) Sastre, G.; Viruela, P. M.; Corma, A. Quantum chemistry calculations on the effect of electron confinement upon the frontier molecular orbitals of ethylene and benzene in sodalite. Implications on reactivity. *Chem. Phys. Lett.* **1997**, *264* (6), 565−572.
(154) Lin, S.; Zhi, Y.; Zhang, W.; Yuan, X.; Zhang, C.; Ye, M.; Xu, S.; Wei, Y.; Liu, Z. Hydrogen transfer reaction contributes to the dynamic evolution of zeolite-catalyzed methanol and dimethyl ether conversions: insight into formaldehyde. *Chin. J. Catal.* **2023**, *46*, 11−27.
(155) Müller, S.; Liu, Y.; Kirchberger, F. M.; Tonigold, M.; Sanchez-Sanchez, M.; Lercher, J. A. Hydrogen transfer pathways during zeolite

catalyzed methanol conversion to hydrocarbons. *J. Am. Chem. Soc.* **2016**, *138* (49), 15994−16003.
(156) Liu, Y.; Kirchberger, F. M.; Müller, S.; Eder, M.; Tonigold, M.; Sanchez-Sanchez, M.; Lercher, J. A. Critical role of formaldehyde during methanol conversion to hydrocarbons. *Nat. Commun.* **2019**, *10* (1), 1462.
(157) Wang, S.; Chen, Y.; Qin, Z.; Zhao, T.-S.; Fan, S.; Dong, M.; Li, J.; Fan, W.; Wang, J. Origin and evolution of the initial hydrocarbon pool intermediates in the transition period for the conversion of methanol to olefins over H-ZSM-5 zeolite. *J. Catal.* **2019**, *369*, 382−395.
(158) Hernandez, E. D.; Jentoft, F. C. Spectroscopic signatures reveal cyclopentenyl cation contributions in methanol-to-olefins catalysis. *ACS Catal.* **2020**, *10* (10), 5764−5782.
(159) Hu, M.; Wang, C.; Gao, X.; Chu, Y.; Qi, G.; Wang, Q.; Xu, G.; Xu, J.; Deng, F. Establishing a link between the dual cycles in methanol-to-olefins conversion on H-ZSM-5: aromatization of cycloalkenes. *ACS Catal.* **2020**, *10* (7), 4299−4305.
(160) Fan, S.; Wang, H.; He, S.; Yuan, K.; Wang, P.; Li, J.; Wang, S.; Qin, Z.; Dong, M.; Fan, W.; Wang, J. Formation and evolution of methylcyclohexene in the initial period of methanol to olefins over H-ZSM-5. *ACS Catal.* **2022**, *12* (20), 12477−12487.
(161) Yang, L.; Wang, C.; Dai, W.; Wu, G.; Guan, N.; Li, L. Progressive steps and catalytic cycles in methanol-to-hydrocarbons reaction over acidic zeolites. *Fundam. Res.* **2022**, *2* (2), 184−192.
(162) Yu, B.; Zhang, W.; Wei, Y.; Wu, X.; Sun, T.; Fan, B.; Xu, S.; Liu, Z. Capture and identification of coke precursors to elucidate the deactivation route of the methanol-to-olefin process over H-SAPO-34. *Chem. Commun.* **2020**, *56* (58), 8063−8066.
(163) Bjørgen, M.; Akyalcin, S.; Olsbye, U.; Benard, S.; Kolboe, S.; Svelle, S. Methanol to hydrocarbons over large cavity zeolites: toward a unified description of catalyst deactivation and the reaction mechanism. *J. Catal.* **2010**, *275* (1), 170−180.
(164) Bjørgen, M.; Olsbye, U.; Kolboe, S. Coke precursor formation and zeolite deactivation: mechanistic insights from hexamethylbenzene conversion. *J. Catal.* **2003**, *215* (1), 30−44.
(165) Wei, Y.; Li, J.; Yuan, C.; Xu, S.; Zhou, Y.; Chen, J.; Wang, Q.; Zhang, Q.; Liu, Z. Generation of diamondoid hydrocarbons as confined compounds in SAPO-34 catalyst in the conversion of methanol. *Chem. Commun.* **2012**, *48* (25), 3082−3084.
(166) Wei, Y.; Yuan, C.; Li, J.; Xu, S.; Zhou, Y.; Chen, J.; Wang, Q.; Xu, L.; Qi, Y.; Zhang, Q.; Liu, Z. Coke formation and carbon atom economy of methanol-to-olefins reaction. *ChemSusChem* **2012**, *5* (5), 906−912.
(167) Goetze, J.; Meirer, F.; Yarulina, I.; Gascon, J.; Kapteijn, F.; Ruiz-Martínez, J.; Weckhuysen, B. M. Insights into the activity and deactivation of the methanol-to-olefins process over different small-pore zeolites as studied with operando UV-vis spectroscopy. *ACS Catal.* **2017**, *7* (6), 4033−4046.
(168) Goetze, J.; Yarulina, I.; Gascon, J.; Kapteijn, F.; Weckhuysen, B. M. Revealing lattice expansion of small-pore zeolite catalysts during the methanol-to-olefins process using combined operando X-ray diffraction and UV-vis spectroscopy. *ACS Catal.* **2018**, *8* (3), 2060−2070.
(169) Van Speybroeck, V.; Hemelsoet, K.; Minner, B.; Marin, G. B.; Waroquier, M. Modeling elementary reactions in coke formation from first principles. *Mol. Simul.* **2007**, *33* (9−10), 879−887.
(170) Hemelsoet, K.; Van Speybroeck, V.; Waroquier, M. A DFT-based investigation of hydrogen abstraction reactions from methylated polycyclic aromatic hydrocarbons. *ChemPhysChem* **2008**, *9* (16), 2349−2358.
(171) Foley, B. L.; Johnson, B. A.; Bhan, A. Kinetic evaluation of deactivation pathways in methanol-to-hydrocarbon catalysis on HZSM-5 with formaldehyde, olefinic, dieneic, and aromatic co-feeds. *ACS Catal.* **2021**, *11* (6), 3628−3637.
(172) Martinez-Espin, J. S.; De Wispelaere, K.; Westgård Erichsen, M.; Svelle, S.; Janssens, T. V. W.; Van Speybroeck, V.; Beato, P.; Olsbye, U. Benzene co-reaction with methanol and dimethyl ether over zeolite and zeotype catalysts: evidence of parallel reaction paths to toluene and diphenylmethane. *J. Catal.* **2017**, *349*, 136−148.
(173) Martinez-Espin, J. S.; Mortén, M.; Janssens, T. V. W.; Svelle, S.; Beato, P.; Olsbye, U. New insights into catalyst deactivation and product distribution of zeolites in the methanol-to-hydrocarbons (MTH) reaction with methanol and dimethyl ether feeds. *Catal. Sci. Technol.* **2017**, *7* (13), 2700−2716.
(174) Martínez-Espín, J. S.; De Wispelaere, K.; Janssens, T. V. W.; Svelle, S.; Lillerud, K. P.; Beato, P.; Van Speybroeck, V.; Olsbye, U. Hydrogen transfer versus methylation: on the genesis of aromatics formation in the methanol-to-hydrocarbons reaction over H-ZSM-5. *ACS Catal.* **2017**, *7* (9), 5773−5780.
(175) Hutchings, G. J.; Gottschalk, F.; Hunter, R. Comments on "kinetic model for methanol conversion to olefins" with respect to methane formation at low conversion. *Ind. Eng. Chem. Res.* **1987**, *26* (3), 635−637.
(176) Hutchings, G. J.; Gottschalk, F.; Hall, M. V. M.; Hunter, R. Hydrocarbon formation from methylating agents over the zeolite catalyst ZSM-5. Comments on the mechanism of carbon-carbon bond and methane formation. *J. Chem. Soc., Faraday Trans. 1* **1987**, *83* (3), 571−583.
(177) Kubelková, L.; Nováková, J.; Jírů, P. Reaction of small amounts of methanol on HZSM-5, Hy and modified Y zeolites. *Stud. Surf. Sci. Catal.* **1984**, *18*, 217−224.
(178) Nováková, J.; Kubelková, L.; Dolejšek, Z. Primary reaction steps in the methanol-to-olefin transformation on zeolites. *J. Catal.* **1987**, *108* (1), 208−213.
(179) Wei, Z.; Chen, Y.-Y.; Li, J.; Wang, P.; Jing, B.; He, Y.; Dong, M.; Jiao, H.; Qin, Z.; Wang, J.; Fan, W. Methane formation mechanism in the initial methanol-to-olefins process catalyzed by SAPO-34. *Catal. Sci. Technol.* **2016**, *6* (14), 5526−5533.
(180) Kirchberger, F. M.; Liu, Y.; Plessow, P. N.; Tonigold, M.; Studt, F.; Sanchez-Sanchez, M.; Lercher, J. A. Mechanistic differences between methanol and dimethyl ether in zeolite-catalyzed hydrocarbon synthesis. *Proc. Natl. Acad. Sci. U. S. A.* **2022**, *119* (4), e2103840119.
(181) Pare, C. W. P.; Rzepka, P.; Hemberger, P.; Bodi, A.; Hauert, R.; van Bokhoven, J. A.; Paunović, V. Formaldehyde-induced deactivation of ZSM5 catalysts during the methanol-to-hydrocarbons conversion. *ACS Catal.* **2024**, *14* (1), 463−474.
(182) Luo, J.; Xiao, T.; Liu, C.; Pan, Y. Recent progress on the involvement of formaldehyde in the methanol-to-hydrocarbons reaction. *ChemSusChem* **2025**, *18* (2), e202400884.
(183) Paunović, V.; Wu, X.; Maggiulli, L.; Ferri, D.; Hemberger, P.; Bodi, A.; van Bokhoven, J. A. The formation, reactivity and transformation pathways of formaldehyde in the methanol-to-hydrocarbon conversion. *Catal. Sci. Technol.* **2024**, *14* (5), 1216−1228.
(184) Wen, W.; Yu, S.; Zhou, C.; Ma, H.; Zhou, Z.; Cao, C.; Yang, J.; Xu, M.; Qi, F.; Zhang, G.; Pan, Y. Formation and fate of formaldehyde in methanol-to-hydrocarbon reaction: in situ synchrotron radiation photoionization mass spectrometry study. *Angew. Chem., Int. Ed.* **2020**, *59* (12), 4873−4878.
(185) Paunović, V.; Hemberger, P.; Bodi, A.; Hauert, R.; van Bokhoven, J. A. Impact of nonzeolite-catalyzed formation of formaldehyde on the methanol-to-hydrocarbons conversion. *ACS Catal.* **2022**, *12* (21), 13426−13434.
(186) Ma, K.; Zhao, S.; Dou, M.; Ma, X.; Dai, C. Enhancing the stability of methanol-to-olefins reaction catalyzed by SAPO-34 zeolite in the presence of CO_2 and oxygen-vacancy-rich ZnCeZrOx. *ACS Catal.* **2024**, *14* (2), 594−607.
(187) Pfriem, N.; Hintermeier, P. H.; Eckstein, S.; Kim, S.; Liu, Q.; Shi, H.; Milakovic, L.; Liu, Y.; Haller, G. L.; Baráth, E.; Liu, Y.; Lercher, J. A. Role of the ionic environment in enhancing the activity of reacting molecules in zeolite pores. *Science* **2021**, *372* (6545), 952−957.
(188) Arora, S. S.; Bhan, A. The critical role of methanol pressure in controlling its transfer dehydrogenation and the corresponding effect

on propylene-to-ethylene ratio during methanol-to-hydrocarbons catalysis on H-ZSM-5. *J. Catal.* **2017**, *356*, 300−306.
(189) Hwang, A.; Kumar, M.; Rimer, J. D.; Bhan, A. Implications of methanol disproportionation on catalyst lifetime for methanol-to-olefins conversion by HSSZ-13. *J. Catal.* **2017**, *346*, 154−160.
(190) Hwang, A.; Bhan, A. Bifunctional strategy coupling Y_2O_3-catalyzed alkanal decomposition with methanol-to-olefins catalysis for enhanced lifetime. *ACS Catal.* **2017**, *7* (7), 4417−4422.
(191) Marchi, A. J.; Froment, G. F. Catalytic conversion of methanol into light alkenes on mordenite-like zeolites. *Appl. Catal., A* **1993**, *94* (1), 91−106.
(192) Marchi, A. J.; Froment, G. F. Catalytic conversion of methanol to light alkenes on SAPO molecular sieves. *Appl. Catal.* **1991**, *71* (1), 139−152.
(193) Wang, H.; Hou, Y.; Sun, W.; Hu, Q.; Xiong, H.; Wang, T.; Yan, B.; Qian, W. Insight into the effects of water on the ethene to aromatics reaction with HZSM-5. *ACS Catal.* **2020**, *10* (9), 5288−5298.
(194) Zhao, X.; Li, J.; Tian, P.; Wang, L.; Li, X.; Lin, S.; Guo, X.; Liu, Z. Achieving a superlong lifetime in the zeolite-catalyzed MTO reaction under high pressure: synergistic effect of hydrogen and water. *ACS Catal.* **2019**, *9* (4), 3017−3025.
(195) Arora, S. S.; Shi, Z.; Bhan, A. Mechanistic basis for effects of high-pressure H_2 cofeeds on methanol-to-hydrocarbons catalysis over zeolites. *ACS Catal.* **2019**, *9* (7), 6407−6414.
(196) DeLuca, M.; Janes, C.; Hibbitts, D. Contrasting arene, alkene, diene, and formaldehyde hydrogenation in H-ZSM-5, H-SSZ-13, and H-SAPO-34 frameworks during MTO. *ACS Catal.* **2020**, *10* (8), 4593−4607.
(197) Liu, G.; Tian, P.; Zhang, Y.; Li, J.; Xu, L.; Meng, S.; Liu, Z. Synthesis of SAPO-34 templated by diethylamine: crystallization process and Si distribution in the crystals. *Microporous Mesoporous Mater.* **2008**, *114* (1), 416−423.
(198) Tian, P.; Li, B.; Xu, S.; Su, X.; Wang, D.; Zhang, L.; Fan, D.; Qi, Y.; Liu, Z. Investigation of the crystallization process of SAPO-35 and Si distribution in the crystals. *J. Phys. Chem. C* **2013**, *117* (8), 4048−4056.
(199) Gao, M.; Li, H.; Yu, J.; Ye, M.; Liu, Z. Quantitative principle of shape-selective catalysis for a rational screening of zeolites for methanol-to-hydrocarbons. *AIChE J.* **2023**, *69* (2), e17881.
(200) Teketel, S.; Westgård Erichsen, M.; Lønstad Bleken, F.; Svelle, S.; Petter Lillerud, K.; Olsbye, U. Shape selectivity in zeolite catalysis. The methanol to hydrocarbons (MTH) reaction. *Catalysis* **2014**, *26*, 179−217.
(201) Zhong, J.; Han, J.; Wei, Y.; Liu, Z. Catalysts and shape selective catalysis in the methanol-to-olefin (MTO) reaction. *J. Catal.* **2021**, *396*, 23−31.
(202) Chen, J.; Li, J.; Wei, Y.; Yuan, C.; Li, B.; Xu, S.; Zhou, Y.; Wang, J.; Zhang, M.; Liu, Z. Spatial confinement effects of cage-type SAPO molecular sieves on product distribution and coke formation in methanol-to-olefin reaction. *Catal. Commun.* **2014**, *46*, 36−40.
(203) Pinilla-Herrero, I.; Olsbye, U.; Márquez-Álvarez, C.; Sastre, E. Effect of framework topology of SAPO catalysts on selectivity and deactivation profile in the methanol-to-olefins reaction. *J. Catal.* **2017**, *352*, 191−207.
(204) Zhang, W.; Chen, J.; Xu, S.; Chu, Y.; Wei, Y.; Zhi, Y.; Huang, J.; Zheng, A.; Wu, X.; Meng, X.; Xiao, F.; Deng, F.; Liu, Z. Methanol to olefins reaction over cavity-type zeolite: cavity controls the critical intermediates and product selectivity. *ACS Catal.* **2018**, *8* (12), 10950−10963.
(205) Yang, M.; Li, B.; Gao, M.; Lin, S.; Wang, Y.; Xu, S.; Zhao, X.; Guo, P.; Wei, Y.; Ye, M.; Tian, P.; Liu, Z. High propylene selectivity in methanol conversion over a small-pore sapo molecular sieve with ultra-small cage. *ACS Catal.* **2020**, *10* (6), 3741−3749.
(206) Ferri, P.; Li, C.; Millán, R.; Martínez-Triguero, J.; Moliner, M.; Boronat, M.; Corma, A. Impact of zeolite framework composition and flexibility on methanol-to-olefins selectivity: confinement or diffusion? *Angew. Chem., Int. Ed.* **2020**, *59* (44), 19708−19715.
(207) Kang, J. H.; Alshafei, F. H.; Zones, S. I.; Davis, M. E. Cage-defining ring: a molecular sieve structural indicator for light olefin product distribution from the methanol-to-olefins reaction. *ACS Catal.* **2019**, *9* (7), 6012−6019.
(208) Han, J.; Liu, Z.; Li, H.; Zhong, J.; Zhang, W.; Huang, J.; Zheng, A.; Wei, Y.; Liu, Z. Simultaneous evaluation of reaction and diffusion over molecular sieves for shape-selective catalysis. *ACS Catal.* **2020**, *10* (15), 8727−8735.
(209) Cnudde, P.; Redekop, E. A.; Dai, W.; Porcaro, N. G.; Waroquier, M.; Bordiga, S.; Hunger, M.; Li, L.; Olsbye, U.; Van Speybroeck, V. Experimental and theoretical evidence for the promotional effect of acid sites on the diffusion of alkenes through small-pore zeolites. *Angew. Chem., Int. Ed.* **2021**, *60* (18), 10016−10022.
(210) Ghysels, A.; Moors, S. L. C.; Hemelsoet, K.; De Wispelaere, K.; Waroquier, M.; Sastre, G.; Van Speybroeck, V. Shape-selective diffusion of olefins in 8-ring solid acid microporous zeolites. *J. Phys. Chem. C* **2015**, *119* (41), 23721−23734.
(211) Cai, D.; Cui, Y.; Jia, Z.; Wang, Y.; Wei, F. High-precision diffusion measurement of ethane and propane over SAPO-34 zeolites for methanol-to-olefin process. *Front. Chem. Sci. Eng.* **2018**, *12* (1), 77−82.
(212) Chen, D.; Rebo, H. P.; Moljord, K.; Holmen, A. Dimethyl ether conversion to light olefins over SAPO-34: deactivation due to coke deposition. *Stud. Surf. Sci. Catal.* **1998**, *119*, 521−526.
(213) Chen, D.; Rebo, H. P.; Holmen, A. Diffusion and deactivation during methanol conversion over SAPO-34: a percolation approach. *Chem. Eng. Sci.* **1999**, *54* (15), 3465−3473.
(214) Hwang, A.; Le, T. T.; Shi, Z.; Dai, H.; Rimer, J. D.; Bhan, A. Effects of diffusional constraints on lifetime and selectivity in methanol-to-olefins catalysis on HSAPO-34. *J. Catal.* **2019**, *369*, 122−132.
(215) Li, Y.; Zhang, M.; Wang, D.; Wei, F.; Wang, Y. Differences in the methanol-to-olefins reaction catalyzed by SAPO-34 with dimethyl ether as reactant. *J. Catal.* **2014**, *311*, 281−287.
(216) Konnov, S. V.; Pavlov, V. S.; Kots, P. A.; Zaytsev, V. B.; Ivanova, I. I. Mechanism of SAPO-34 catalyst deactivation in the course of MTO conversion in a slurry reactor. *Catal. Sci. Technol.* **2018**, *8* (6), 1564−1577.
(217) Khare, R.; Millar, D.; Bhan, A. A mechanistic basis for the effects of crystallite size on light olefin selectivity in methanol-to-hydrocarbons conversion on MFI. *J. Catal.* **2015**, *321*, 23−31.
(218) Park, T.-Y.; Froment, G. F. Kinetic modeling of the methanol to olefins process. 1. model formulation. *Ind. Eng. Chem. Res.* **2001**, *40* (20), 4172−4186.
(219) Kumar, P.; Thybaut, J. W.; Svelle, S.; Olsbye, U.; Marin, G. B. Single-event microkinetics for methanol to olefins on H-ZSM-5. *Ind. Eng. Chem. Res.* **2013**, *52* (4), 1491−1507.
(220) Olsbye, U.; Bjørgen, M.; Svelle, S.; Lillerud, K.-P.; Kolboe, S. Mechanistic insight into the methanol-to-hydrocarbons reaction. *Catal. Today* **2005**, *106* (1), 108−111.
(221) Chang, C. D. A kinetic model for methanol conversion to hydrocarbons. *Chem. Eng. Sci.* **1980**, *35* (3), 619−622.
(222) Bos, A. N. R.; Tromp, P. J. J.; Akse, H. N. Conversion of methanol to lower olefins. kinetic modeling, reactor simulation, and selection. *Ind. Eng. Chem. Res.* **1995**, *34* (11), 3808−3816.
(223) Chen, D.; Grønvold, A.; Moljord, K.; Holmen, A. Methanol conversion to light olefins over SAPO-34: reaction network and deactivation kinetics. *Ind. Eng. Chem. Res.* **2007**, *46* (12), 4116−4123.
(224) Ying, L.; Yuan, X.; Ye, M.; Cheng, Y.; Li, X.; Liu, Z. A seven lumped kinetic model for industrial catalyst in DMTO process. *Chem. Eng. Res. Des.* **2015**, *100*, 179−191.
(225) Remi, J. C. S.; Lauerer, A.; Chmelik, C.; Vandendael, I.; Terryn, H.; Baron, G. V.; Denayer, J. F. M.; Kärger, J. The role of crystal diversity in understanding mass transfer in nanoporous materials. *Nat. Mater.* **2016**, *15* (4), 401−406.
(226) Peng, S.; Xie, Y.; Wang, L.; Liu, W.; Li, H.; Xu, Z.; Ye, M.; Liu, Z. Exploring the influence of inter- and intra-crystal diversity of surface barriers in zeolites on mass transport by using super-resolution

https://doi.org/10.1021/jacs.4c12145
J. Am. Chem. Soc. 2025, 147, 11585−11607

microimaging of time-resolved guest profiles. *Angew. Chem., Int. Ed.* **2022**, *61* (30), e202203903.
(227) Macdonald, D. D. The mathematics of diffusion. Transient techniques in electrochemistry. *Springer US* **1977**, 47−67.
(228) Peng, S.; Gao, M.; Li, H.; Yang, M.; Ye, M.; Liu, Z. Control of surface barriers in mass transfer to modulate methanol-to-olefins reaction over SAPO-34 zeolites. *Angew. Chem., Int. Ed.* **2020**, *59* (49), 21945−21948.
(229) Krishna, R.; Wesselingh, J. A. The Maxwell-Stefan approach to mass transfer. *Chem. Eng. Sci.* **1997**, *52* (6), 861−911.
(230) Li, H.; Ye, M.; Liu, Z. A multi-region model for reaction-diffusion process within a porous catalyst pellet. *Chem. Eng. Sci.* **2016**, *147*, 1−12.
(231) Hansen, N.; Krishna, R.; van Baten, J. M.; Bell, A. T.; Keil, F. J. Analysis of diffusion limitation in the alkylation of benzene over H-ZSM-5 by combining quantum chemical calculations, molecular simulations, and a continuum approach. *J. Phys. Chem. C* **2009**, *113* (1), 235−246.

https://doi.org/10.1021/jacs.4c12145
J. Am. Chem. Soc. 2025, 147, 11585−11607